1 **Mitochondrial ascorbate synthesis acts as a pro-oxidant pathway and**

2 **down-regulate energy supply in plants**

3 Authors

4 Luis Miguel Mazorra Morales[1b], Gláucia Michelle Cosme Silva[1a], Diederson Bortolini Santana[a],

5 Saulo F. Pireda[c], Antonio Jesus Dorighetto Cogo[c], Angelo Schuabb Heringer[d], Tadeu dos Reis de

6 Oliveira[c], Ricardo S. Reis[d], Luís Alfredo dos Santos Prado[c], André Vicente de Oliveira[a], Vanildo

7 Silveira[d], Maura Da Cunha[c], Claudia F. Barros[e], Arnoldo R. Facanha[c], Pierre Baldet[f], Carlos Bartoli[g],

8 Marcelo Gomes da Silva*[b], Jurandi Gonçalves de Oliveira*[a]

9 *corresponding authors

10 [1] Both authors contributed equally to this wok

11 Authors affiliations

12 [a] Laboratório de Melhoramento Genético Vegetal, Centro de Ciências e Tecnologias Agropecuárias,
13 Universidade Estadual do Norte Fluminense Darcy Ribeiro (UENF), Campos dos Goytacazes, Rio de
14 Janeiro, CEP 28013-602, Brazil

15 [b] Laboratório de Ciências Físicas, Centro de Ciências Tecnologia, Universidade Estadual do Norte
16 Fluminense Darcy Ribeiro (UENF), Campos dos Goytacazes, Rio de Janeiro, CEP 28013-602, Brazil.

17 [c] Laboratório de Biologia Celular e Tecidual, Centro de Biociências e Biotecnologia, Universidade
18 Estadual do Norte Fluminense Darcy Ribeiro (UENF), Campos dos Goytacazes, Rio de Janeiro, CEP
19 28013-602, Brazil.

20 [d] Laboratório de Biotecnologia, Universidade Estadual do Norte Fluminense "Darcy Ribeiro"
21 (UENF), Campos dos Goytacazes, RJ, Brazil

22 [e] Laboratório de Botânica Estrutural, Instituto de Pesquisas Jardim Botânico do Rio de Janeiro –
23 IPJBRJ, Brazil

24 [f] Institut National de la Recherche Agronomique, Université Bordeaux 1, Université Victor Ségalen-
25 Bordeaux 2, Institut Fédératif de Recherche 103, Unité Mixte de Recherche 619 sur la Biologie du
26 Fruit, Centre de Recherche Institut National de la Recherche Agronomique de Bordeaux, BP 81,
27 33883 Villenave d'Ornon cedex, France

28 [g] Instituto de Fisiología Vegetal, Facultad Ciencias Agrarias y Forestales, Universidad Nacional de La
29 Plata, CCT-CONICET, cc327 1900 La Plata, Argentina

30

31   *ABSTRACT*

32   Attempts to improve the ascorbate (AsA) content of plants are still dealing with the limited

33   understanding of why exists a wide variability of this powerful anti-oxidant molecule in different

34   plant sources, species and environmental situations. In plant mitochondria, the last step of AsA

35   synthesis is catalyzed by the enzyme L-galactone-1,4-lactone dehydrogenase (L-GalLDH). By using

36   GalLDH-RNAi silencing plant lines, biochemical and proteomic approaches, we here discovered

37   that, in addition to accumulate this antioxidant, mitochondria synthesize AsA to down-regulate the

38   respiratory activity and the cellular energy provision. The work reveals that the AsA synthesis

39   pathway within mitochondria is a branched electron transfer process that channels electrons

40   towards the alternative oxidase, interfering with conventional electron transport. It was

41   unexpectedly found that significant hydrogen peroxide is generated during AsA synthesis, which

42   affects the AsA level. The induced AsA synthesis shows proteomic alterations of mitochondrial

43   and extra-mitochondrial proteins related to oxidative and energetic metabolism.   The most

44   identified proteins were known components of plant responses to high light acclimation,

45   programmed cell death, oxidative stress, senescence, cell expansion, iron and phosphorus

46   starvation, different abiotic stress/pathogen attack responses and others. We propose that

47   changing the electron flux associated with AsA synthesis might be part of a new mechanism by

48   which the L-GalLDH enzyme would adapt plant mitochondria to fluctuating energy demands and

49   redox status occurring under different physiological contexts.

50

51   *INTRODUCTION*

52   In plants, the mitochondrial electron transport chain (mETC) consists of a series of electron

53   transporters that function to oxidize reducing equivalents, NADP(H) and $FADH_2$ (Schertl and Braun,

54   2014). A widely accepted model about the electron transfer is that the electrons normally enter

55   via complex I (NADH:ubiquinone oxidoreductase) or through a diversity of "alternative" NAD(P)H

56   dehydrogenases using flavin mononucleotide (FMN) as electron acceptor (Pineau et al., 2005).

57   Alternatively, complex II (succinate:ubiquinone oxidoreductase) and other dehydrogenases such as

58   glyceraldehyde 3-phosphate dehydrogenase (G3-PDH), the "electron transfer flavoprotein-

59   ubiquinone oxidoreductase" (ETFQ-OR) and the proline dehydrogenase (ProDH) supply electrons

60   to mETC but via flavin dinucleotide (FAD) (Sweetlove et al., 2010). These oxidation reactions are all

61   coupled to reduction of the ubiquinone (UQ) to ubiquinol (UQH$_2$) (Schertl and Braun, 2014).

62   To accomplish ubiquinol re-oxidation, two routes have been proposed. The cytochrome c oxidase

63   pathway (COX), in which electrons in UQH$_2$ are then passed to complex III (ubiquinone:cytochrome

64   c oxidoreductase), which reduces cytochrome c (Cytc) and oxidizes UQH$_2$ and subsequently the

65   reduced Cytc is re-oxidized by complex IV (cytochrome c oxidase) with dependence of electron

66   reduction of O$_2$ to H$_2$O (Millar et al., 2011). The other, the so-called "alternative" oxidase pathway

67   (AOX), directly oxidizes UQH$_2$ coupled with the reduction of O$_2$ to H$_2$O (Vanlerberghe, 2013). Thus,

68   the AOX introduces a branch in the mETC and consequently a regulatory point that allows the

69   partition of electrons between both pathways.

70   The electrons channeled via respiratory complexes (I, III and IV) are coupled to the pumping of H$^+$

71   through the inner-mitochondrial membrane (Millar et al., 2011). Pumping of H$^+$ results in a

72   transmembrane proton gradient, which is required for generation of adenosine triphosphate (ATP)

73   from ADP and Pi via complex V (H$^+$-ATP synthase), a process termed as oxidative phosphorylation.

74   The plant mitochondrial electron transport greatly depends upon AOX pathway. Indeed, the AOX

75   protein is the most highly regulated component of mETC at transcriptional and translational level

76   (Vanlerberghe et al., 2016; Dahal and Vanlerberghe, 2017). When ATP demand is low, ATP

77   synthesis needs to be decreased and the electrons would flow via AOX pathway, it bypasses the

78   H$^+$-pumping protein complexes III and IV, reducing the potential of mitochondrial ATP production

79   (Wagner & Wagner, 1995; Millar et al., 2011; Vanlerberghe, 2013). For example, high AOX

80   pathway in light would act in coordination with photosynthesis (an ATP source) to optimize energy

81   metabolism (Nunes-Nesi et al., 2011).

82   Other role for AOX pathway is to avoid the over-flux through COX pathway and consequently ROS

83   over-production (Vanlerberghe et al., 2016; Dahal and Vanlerberghe, 2017). When ATP supply

84   through COX pathway is uncoupled from energy demand, it leads to the over-reduction of mETC

85   and the formation of partially reduced forms of electron carriers such as flavins (FAD, FMN) and

86   ubiquinone, which can potentially react with oxygen (O$_2$) to form reactive oxygen species (ROS),

87   e.g. O$_2^-$, H$_2$O$_2$, ^{1}O$_2$ (Mailloux and Harper, 2011) . If ROS are not effectively scavenged, they would

88   generate oxidative damage (Noctor and Foyer, 2016). ROS can also have positive signaling roles at

89   low concentrations and therefore control of ROS load by AOX has been involved in ROS signaling,

90   programmed cell death, abiotic/biotic stress tolerance and plant growth (Vanlerberghe, 2013).

3

91   Ascorbate is an abundant molecule in plants, which plays multiple roles as antioxidant, pro-

92   oxidant and co-factor for multiple enzymes in plants and mammals reviewed in Smirnoff, 2018.

93   AsA is ultimately synthesized by plant mitochondria through another dehydrogenase, the L-

94   galactone-1,4-lactone dehydrogenase (L-GalLDH EC 1.3.2.3). This enzyme is a FAD-dependent

95   dehydrogenase that catalyzes the L-Galactone-1,4-lactone (L-GalL) oxidation. The plant L-GalLDH

96   enters electrons directly to mETC through cytochrome c (Bartoli et al., 2000). L-GalLDH expression

97   and AsA synthesis are under diurnal control (Tamaoki et al., 2003) and are up-regulated by light in

98   an AOX-dependent manner (Bartoli et al., 2006). Conversely, L-GalDH expression and AsA

99   synthesis are down-regulated in dark and with ageing (Tamaoki et al., 2003). Beyond its roles in

100   AsA synthesis and in the assembly of complex I (Schertl et al., 2012), the significance of L-GalLDH

101   as component of mETC is still unclear.

102   The analysis of several AsA-deficient mutants with defects in key points of AsA biosynthesis

103   pathway highlights different roles of AsA through plant lifecycle. AsA-biosynthesis mutants have

104   showed alterations in flowering and senescence (Kotchoni et al., 2009), enhanced sensitivity to

105   high light, salt, UV-B radiation and extreme temperatures (Smirnoff, 2011), biotrophic pathogen

106   resistance (Mukherjee et al., 2010), tolerance to postsubmergence reoxygenation (Yuan et al.,

107   2017); hormonal control (Foyer et al., 2007), sucrose and iron uptake (Grillet et al., 2014) and

108   plant growth (Alhagdow et al., 2007). Interestingly, several physiological effects seemed to be

109   independent of AsA deficiency (Smirnoff, 2018); however, the causes of this independence are

110   unclear. The analysis of AsA synthesis-altered plants, specifically in the mitochondrial L-GalLDH

111   expression, would offer a valuable tool to explore the roles of the last step of AsA synthesis into

112   mitochondria and the impact on plant growth, development and stress tolerance.

113   We here revealed that mitochondrial AsA synthesis down-regulates energy supply and generates

114   hydrogen peroxide accumulation. This pathway is a branched electron transfer process that

115   channels electrons towards alternative oxidase. The proteomic of tissues with enhanced AsA

116   synthesis reveals proteins related to oxidative and energetic homeostasis, suggesting that

117   mitochondrial AsA synthesis leads to a global switch in redox and energy loads. These findings

118   establish a new pro-oxidant function for AsA synthesis beyond producing this powerful anti-

119   oxidant.

120

4

121   ***RESULTS***

122   *The alternative respiration is modulated by mitochondrial ascorbate synthesis*

123   To answer the question how the L-GalLDH enzyme affects the mitochondrial electron transport

124   chain (mETC), we examined the effects of respiratory inhibitors on mitochondrial respiration of

125   RNAi-plant lines harboring silenced L-GalLDH activity. As expected, the mixture of AOX and COX

126   inhibitors (5 mM SHAM and 3 mM NaN₃) decreased the oxygen uptake rate of leaf mitochondria

127   purified from wild type plants and L-GalLDH-RNAi plant lines (Figure 1A). Residual oxygen uptakes

128   were observed in presence of both inhibitors. When leaf mitochondria were pre-treated with the

129   L-GalLDH substrate (5 mM L-GalL), absolute respiration was greatly reduced and was not sensitive

130   to the mixture of both inhibitors in wild type mitochondria. Nonetheless, a significant blockage of

131   respiration occurred in the L-GalL-treated leaf mitochondria from L-GalLDH-RNAi plant lines

132   (Figure 1A), which suggest that part of the AOX and COX pathways is active. The western blot

133   analysis showed lower levels of L-GalLDH protein abundance in both L-GalLDH-RNAi plant lines

134   (~21% and ~63% of Wt for 8-14 and 5-13 plant lines, respectively), which resulted in decreased L-

135   GalLDH activity (Figure 1B). Notably, the level of L-GalLDH suppression but not the enzyme activity

136   was more marked in the L-GalLDH-RNAi line 8-14 as compared to 5-13 line.

137   To further explore the causes of the differences in respiratory rates, we analyzed the flow of

138   electrons through the AOX pathway in the presence of L-GalLDH substrate. Clearly, the Figure 1C

139   shows that leaf mitochondria of the L-GalLDH-RNAi plants had significant alternative respiration ~9

140   nmol O₂/mg protein was resistant to NaN₃ and sensitive to SHAM in presence of L-GalL. However,

141   it was not detected in wild type mitochondria (Figure 1C). The SDS-PAGE electrophoresis of

142   mitochondrial proteins and subsequent inmunobloting with anti-AOX antibodies allowed the

143   detection of a band of ~66 kDa in addition to trace level of ~33 kDa protein. However, when the

144   samples for SDS-PAGE electrophoresis were prepared with the reducing agent, 2-

145   mercaptoethanol, into the sample buffer, the band of ~33 kDa intensified and that of ~66 kDa

146   virtually disappeared (Data not shown). Because the 2-mercaptoethanol reduces disulfide bond

147   linkages within proteins, the presence of 33 kDa AOX protein could result from the break of the

148   intermolecular disulfide bond in the 66 kDa AOX dimer by this reducing agent. Consistently,

149   previous works showed the existence of a single 33 kDa AOX isoform in tomato mitochondria

150   (Holtzapffel et al., 2002) and the dimerization of the 33 kDa AOX isoform by the oxidant, diamide

151   (Holtzapffel et al., 2002). Most importantly was that the quantification by densitometry of

5

152   independent gels (with equal loading of proteins, supplementary data I) showed higher amount of

153   AOX (for both the 66 kDa and 33 kDa AOX) in wild type plants while it was lower in L-GalLDH-RNAi

154   plant lines (Figure 1D). Taken together, these data suggest that the AOX molecules in wild type

155   mitochondria are significantly inhibited by L-GalL due to the L-GalLDH activity. In the plant lines,

156   the suppression of L-GalLDH enzyme could, in turn, prevent AOX inhibition by L-GalL.

157   Interestingly, the 8-14 plant line, which has the higher L-GalLDH suppression (Figure 1B) showed

158   the lower level of oxidized AOX (Figure 1D).

159   We examined the respiratory capacity of mitochondria purified from heterotrophic tissues (fruits)

160   of other plant species and using other respiratory substrates and inhibitors. The mitochondrial

161   preparations of fruit purified with a Percoll density-gradient method had intact mitochondria

162   (≥80% integrity). The content of mitochondria (based on mitochondrial protein) ranged from 1 to

163   3.4 mg protein. The oxygen uptake of papaya, strawberry and tomato fruit mitochondria was

164   blocked by respiratory inhibitors (supplementary data IIA). However, respiration was insensitive to

165   inhibitors in the presence of L-GalL (supplementary data IIA). Moreover, when energizing

166   mitochondria with other substrates that enter electrons through complexes I (malate, glutamate)

167   or II (succinate), the alternative respiration was blocked by L-GalL (supplementary data IIB).

168   Clearly, the insensitivity of oxygen uptake to inhibitors (supplementary data IIA) and the loss of

169   alternative respiration in presence of L-GalL (supplementary data IIB) were responses in fruit

170   mitochondria that resembled to those found in wild type tomato leaf mitochondria treated with L-

171   GalL (Figure 1A and 1C). It supports the hypothesis of that the L-GalLDH activity down-regulates

172   mitochondrial electron flux by inhibiting the alternative oxidase pathway. Clearly, this is a general

173   effect in both autotrophic and heterotrophic plant tissues.

174   To get further insights about the mechanism inactivating AOX pathway, we adopt papaya fruit

175   mitochondria as model because their ability to synthesize AsA and the significant bulk of active

176   mitochondria with high AOX capacity that can be easily obtained our results here and (Oliveira et

177   al., 2015). Respiration and ascorbate production of papaya mitochondria were stimulated by

178   increasing L-GalL concentrations up to about 5mM. Higher concentrations were progressively

179   inhibitory, being the respiratory activity more sensitive to the inhibition by the substrate

180   concentration (supplementary data III).

181   *The alternative oxidase but not the Cytc oxidase is critical for AsA biosynthesis*

182　By using inhibitors that target specific points in the mETC, we analyzed the possible role of

183　terminal oxidases during mitochondrial AsA synthesis. The current Bartoli's model explaining

184　mitochondrial AsA synthesis implies that Cytc and Cytc oxidase are absolute requirements for AsA

185　production (Bartoli et al., 2000). As Cytc oxidase re-oxidizes Cytc quickly, the L-GalLDH activity,

186　which was measured as rate of Cytc reduction, is assayed in presence of Cytc oxidase inhibitor. It

187　was confirmed that the treatment of mitochondria with the inhibitor of Cytc oxidase (NaN_3, azyde)

188　led to over-accumulation of reduced Cytc (~6 µmol cytc.min^{-1}mg $protein^{-1}$, Figure IIB), consistent

189　with a lower Cytc re-oxidation by this terminal oxidase. However, azyde-treated mitochondria still

190　maintained a little capacity to synthesize ascorbate (~0.35 µg AsA mg $protein^{-1}$, Figure IIA). This

191　suggested that part of AsA synthesis could be independent of Cytc oxidase. On the other hand, the

192　addition of the inhibitor of AOX pathway (SHAM) affected drastically the Cytc reduction by L-GalL

193　(<1 µmol cytc.min^{-1}mg $protein^{-1}$, Figure IIB), and provoked a very low level of AsA content (Figure

194　IIA), it suggests that SHAM limits electron flux through Cytc.

195　　As AOX gene expression and capacity increase during papaya fruit ripening (Oliveira et al.,

196　2015),we comparatively analyzed the L-GalLDH activity between green-mature and fully ripe

197　papaya fruit. The mitochondria from ripe fruit showed lower L-GalLDH activity but had increased

198　AsA synthesis capacity (Figure IIC).

199　In addition, other inhibitors also showed significant effects during AsA synthesis. Mitochondria

200　treated with antimycin A, an inhibitor of complex III, showed the higher value of Cytc reduction (~7

201　µmol cytc.min^{-1}mg $protein^{-1}$) (Figure IIB) and favored AsA synthesis (Figure IIA). Moreover, when

202　complex I was inhibited with rotenone, Cytc reduction and AsA synthesis were still maintained at

203　levels similar to control (Figures IIB and IIA). By contrast, the DPI, an inhibitor of flavin-oxidases,

204　affected markedly Cytc reduction and AsA synthesis (Figures IIB and IIA).

205　*Cytc oxidase is a main factor affecting FAD recycling during AsA synthesis*

206　We followed changes in fluorescence of exogenously supplemented FAD in the presence of L-GalL

207　and then assessed the effect of inhibitors on such changes. It was recorded a variation of FAD

208　fluorescence (about 2500 Units) following incubation with L-GalL (Figure 2D). It indicates that FAD

209　redox state changes during AsA synthesis. All inhibitors tested in this study decreased the effect of

210　L-GalL in FAD fluorescence, having the Cytc oxidase inhibitor, azyde, the highest effect (Figure 2D).

7

211   These data may suggest that the FAD redox state during AsA synthesis is basically controlled by

212   Cytc oxidase, but other respiratory components could be also involved, albeit indirectly.

213   *Mitochondrial uncoupling and ROS over-production are associated with low AOX capacity during*

214   *AsA synthesis*

215   Given that alterations of mETC and AOX pathway may affect the pumping of H^+ and the

216   mitochondrial coupling (Millar et al., 2011), we explored if mitochondrial oxidative

217   phosphorylation is also affected during AsA synthesis. As expected, there was a 19% of membrane

218   depolarization (based on the respiratory increase induced by the uncoupling agent, CCCP) in

219   NADH-respiring mitochondria. However, mitochondrial respiration was insensitive to CCCP in

220   presence of L-GalL (Table I), suggesting that the generation of the proton gradient is affected.

221   Moreover, both the phosphorylation efficiency, measured as ADP:O ratio and the mitochondrial

222   coupling efficiency, determined as RCR, decreased in presence of L-GalL (Table I). Intriguingly,

223   these L-GalL-dependent alterations correlated with higher H^+-ATPase activity of complex V and an

224   unexpected higher mitochondrial capacity to reduce NAD^+ into NADH (Table I). As the ubiquinone

225   redox state and the mitochondrial energy production are regulated by AOX pathway

226   (Vanlerberghe, 2013), we analyzed possible changes in ubiquinone redox state and the

227   mitochondrial ability to synthesize ATP. It was noted that, in the presence of L-GalL, the

228   mitochondrial capacity to maintain UQ in its reduced state (UQH_2) enhanced (about three times

229   more reduced ubiquinone in the L-GalL treatment than in control). Besides, the mitochondrial ATP

230   synthesis capacity was inhibited by L-GalL (Table I). These results suggest that AsA synthesis could

231   cause the over-reduction of mETC and UQ pool, resulting in a decrease (~20%) in ATP synthesis

232   capacity.

233   As AOX is an important ROS scavenger, we hypothesized that the inactivation of AOX pathway

234   during AsA synthesis would enhance ROS. By measuring the H_2O_2 level, using the Amplex Red

235   method, an increased H_2O_2 formation was detected within 5-15 min following incubation of

236   mitochondria with L-GalL, having maximal H_2O_2 increases between 5-20 mM L-GalL whereas

237   response was extremely low or non-detected at concentrations below 5 mM L-GalL

238   (supplementary data IV).

239   We explored the possible sources of mitochondrial ROS during AsA synthesis. Figure IIIA shows the

240   increase in H_2O_2 fluorescence (~50% above control) in mitochondria treated with 5mM L-GalL. This

241 H_2O_2 fluorescence was maintained by AOX inhibitor (SHAM) whereas it was slightly higher than

242 control in presence of Cytc oxidase inhibitor (azyde). Unexpectedly, relative H_2O_2 fluorescence was

243 not further increased with the respiratory inhibitors rotenone (complex I), antimycin A (complex

244 III), and DPI (flavin-oxidase inhibitor) (Figure IIIA).

245 The H_2O_2 production was verified *in vivo* by staining with CM-H_2DCFDA (DCF), a probe for

246 intracellular H_2O_2 detection and simultaneously mark with the mitochondria-selective probe

247 MitoTracker Red CMXRos (Molecular Probes) using confocal microscopy (Figure IIIB). It was found

248 a green DCF signal that co-localized with MitoTracker Red in small (< 1µM diameter) circular-

249 shaped structures, being the DCF signal more intense in the L-GaL-treated tissue (Figure IIIB). It

250 corroborates that H_2O_2 was produced inside the mitochondria. Consistently, we found that the *in*

251 *vivo* ROS staining was still detected in the presence of inhibitor of AOX, slightly decreased with

252 Cytc oxidase´s inhibitor but almost fully disappeared in fruit tissue treated with antimycin A,

253 rotenone and DPI (Figure IIIB). *In vivo* mitochondrial activity in fruit tissue was confirmed by

254 observing the depletion of MitoTracker Red and DCF signals in presence of the mitochondrial

255 uncoupler, CCCP (Data not shown).

256 We also demonstrate the lower production of H_2O_2 in fruit mitochondria from L-GalLDH-RNAi

257 plant lines, which was consistent with an increased AOX respiration during AsA synthesis

258 (supplementary data V). However, despite these mitochondria showed decreased L-GalLDH

259 activity (lower Cytc reduction rate), their abilities to produce AsA and alter FAD redox status were

260 similar to that of wild type fruit mitochondria (supplementary data V). It suggests that AOX

261 pathway may sustain AsA synthesis in mitochondria with low L-GalLDH activity by reducing H_2O_2

262 level.

263 To further examine the role of alternative respiration during AsA synthesis, we performed an

264 opposite experiment in which the AOX is previously activated before the treatment with L-GalL. To

265 this, mitochondria were firstly treated with pyruvate, a known allosteric AOX activator, and

266 subsequently L-GalL was added to inhibit alternative respiration. Surprisingly, the AOX respiration

267 (7.6 nmol O_2 mg min^{-1}protein^{-1}) was not inhibited in the presence of pyruvate (supplementary data

268 VI). Moreover, this lack of inhibitory effect was not related to lower L-GalLDH activity given that its

269 capacity to reduce Cytc remains in presence of pyruvate. However, the higher AOX capacity

270 correlates with lower H_2O_2 production and enhanced AsA synthesis (supplementary data VI).

271   The possibility of that AsA synthesis leads to shifts in the overall functional status of cell was

272   tested by performing a comparative proteomic analysis between untreated and L-GalL-treated

273   papaya fruit tissue. Of the set of 53 proteins identified, 24 (45%) and 29 (55%) were up-regulated

274   and down-regulated by L-GalL, respectively (Table II). Possible roles of these proteins will be

275   discussed later with regards to an involvement of AsA synthesis in ROS and energy metabolism as

276   well as in the plant responses to abiotic and biotic stresses.

277   *Regulation of seedling emergence by L-GalLDH is associated with altered ATP content*

278   To get further insights about the physiological role of L-GalLDH on seedling establishment (an

279   energy-demanding process) , we evaluated AsA synthesis and ATP content in both L-GalLDH-RNAi

280   lines and wild type in germinating seeds and in seedlings that reach the autotrophy capacity. Wild

281   type and L-GalLDH-RNAi seedlings showed similar ability to synthesize AsA, but, wild type ones

282   contain less ATP in dark (Figure 4A). Interestingly, wild type germinating seeds also had a little less

283   ATP content (data not shown). Treatment of seeds with L-GalL inhibited wild type seedling

284   emergence and consequently, they showed shorter seedlings one-week post germination (Figure

285   4B). However, this inhibitory effect of L-GalL was not evident in L-GalLDH-RNAi lines and these

286   seedlings elongated faster (Figure 4B). Under the growth conditions used in the experiment, these

287   differences in size between wild type and plant lines disappeared when seedlings became larger.

288   In fact, at 30-days-old stage, wild type seedlings had higher size (Figure 4B). Nonetheless, carbon

289   dioxide fixation and biomass were comparable between wild type and L-GalLDH-RNAi plant lines

290   at 30 days after germination (Figure 4C).

291   **DISCUSSION**

292   Over many years, it has been believed that plants synthesize AsA basically to produce this

293   powerful antioxidant molecule, which has multiple functions (Smirnoff, 2018). The localization of

294   the L-GalLDH enzyme within mitochondria has supported the obvious paradigm that AsA synthesis

295   exists for producing AsA, which promotes ROS scavenging. We unexpectedly found that AsA

296   synthesis triggers ROS content and down-regulates energy supply. Most specifically, the electron

297   flux derived from L-GalLDH activity is poorly used for the generation of proton gradient and

298   consequently ATP supply. Instead, AsA synthesis interferes with the conventional electron flux

299   associated with the oxidation of reducing equivalents (NADH/FADH$_2$). Surprisigly, this inhibitory

300   effect of the respiratory flux had an unknown characteristic in plants; it is the possibility of

301   activation of a reverse electron flux during AsA synthesis. Therefore, a novel perspective about the

302   bioenergetics of plant mitochondria mayarise: Plants might use the AsA synthesis not only to

303   accumulate this antioxidant but also to induce a new manner to alter the mitochondrial

304   respiratory activity and their redox balance.

305   Unexpectedly, we also see that the known mitochondrial AsA synthesis pathway, which transfers

306   electrons through Cytc (Bartoli et al., 2000) can also transfer electrons towards ubiquinone. It was

307   concluded that AsA synthesis pathway is branched and can function without the need of Cytc

308   oxidase activity. Data show that FAD, which is an electron carrier for L-GalLDH (Leferink et al.,

309   2009) might be enrolled in the electron transfer. Intriguingly, complex II also requires FAD as

310   internal electron carrier for reducing ubiquinone (Schertl and Braun, 2014) and the proteomic

311   analysis revealed a down-regulation of subunit 5 of complex II , which has unknown function so far

312   in plants (Huang and Millar, 2013) but in yeast is required for FAD incorporation (Hao et al., 2009).

313   These facts may suggest that AsA synthesis down-regulates the respiratory transport by interfering

314   with the electron entry through complex II. The existence of a branched AOX-dependent pathway

315   that would interact with the complex II during AsA synthesis may have practical implications. If

316   electrons derived from AsA synthesis can flow via FAD towards the ubiquinone without passing

317   through Cytc, new alternative assays for quantifying L-GalLDH activity might be developed.

318   Similarly to the demonstrated role of AsA synthesis, the AOX pathway can also decline ATP

319   production; however, the later pathway does not reduce the mitochondrial capacity to utilize

320   reducing equivalents (Schertl and Braun, 2014). This difference may be strongly linked with the

321   close inter-relationship between AOX and L-GalLDH expressions (Bartoli et al., 2006). Likely, when

322   plants need to decrease mitochondrial ATP generation, the L-GalLDH enzyme could be expressed

323   to inhibit the respiratory electron flux unlike the AOX pathway, which maintains a significant part

324   of such flux intact, contributing to energy loss. Therefore, the AsA synthesis may be activated to

325   avoid the loss of energy when the need for mitochondrial ATP is low.

326   Our study also shows that the generation of hydrogen peroxide (H_2O_2) during AsA synthesis is

327   crucial for determining AsA level. Paradoxically, AsA is needed for H_2O_2 elimination (Smirnoff,

328   2018) and L-GalLDH and AOX activities are sensitive to H_2O_2 (Leferink et al., 2009). Likely, H_2O_2 also

329   plays a role in inactivating AOX pathway during AsA synthesis. AOX inactivation occurs by the

330   formation of a disulfide bridge between the two cysteine residues in the AOX dimer under

331   oxidizing conditions (Kühn et al., 2015) and it has been proposed as a regulatory mechanism for

11

332   AOX activity (Selinski et al., 2018). AOX plays a role in minimizing ROS load in plants (Dahal and

333   Vanlerberghe, 2017), which may explain why AOX activity showed to be necessary for AsA

334   synthesis and L-GalLDH activity. An excessive hydrogen peroxide level during AsA synthesis might

335   be prevented by coordinated AOX and L-GalLDH protein expressions. In line with this hypothesis,

336   previous results showed a synergism between AOX expression and AsA accumulation in

337   Arabidopsis plants under light (Bartoli et al., 2006). Accordingly, AOX pathway may function to

338   protect plants from the pro-oxidant effect of AsA synthesis.

339   We also hypothesized that the H_2O_2 coming along with AsA synthesis may play a role in defining

340   cell's redox status. Mitochondria can exert a strong control over the redox balance of the cell

341   (Noctor et al., 2007). As a signal molecule, the H_2O_2 produced during AsA synthesis would diffuse

342   to the extra-mitochondrial environment, being a major regulator of redox signaling and protein

343   expression. Our proteomic data revealed regulations of ROS-related enzymes beyond

344   mitochondria during AsA synthesis. Notably, the cytosolic ascorbate peroxidase (cAPX), which

345   utilizes AsA and hydrogen peroxide as substrates (Davletova et al., 2005) was highly responsive.

346   Most of the identified proteins were previously involved in regulatory redox cascades related with

347   hormonal signaling, defense/detoxification, protein folding and transcriptional/translational

348   regulation, membrane/protein trafficking and degradation, programmed cell death (PCD), fruit

349   ripening as well as in stress responses to high light, hypoxia, drought, iron storage, sulfur

350   metabolism and phosphorus starvation (Westlake et al., 2015). The whole picture is consistent

351   with the hypothesis of that these changes of cellular redox state are involved in a retrograde signal

352   transduction associated with mitochondrial AsA synthesis.

353   In addition, retrograde signal associated with AsA synthesis may be regulating sugar and lipid

354   catabolism and cytosolic ATP provision. We note regulations of enzymes linked with extra-

355   mitochondrial ATP generation through glycolysis and sugar metabolism in cytosol and/or cell wall.

356   Pyruvate kinase, phosphoenolpyruvate carboxykinase, threonine aldolase, fructokinase, α-

357   galactosidase, trehalose-6-phosphate synthase and polygalacturonase, which were identified in

358   the proteomic, have been implicated (Schluepmann et al., 2003; Umbach et al., 2006).

359   Consistently, AsA-related mutants present altered sugar metabolism (Alhagdow et al., 2007) and

360   our results showed effects on initial growth and ATP content. AsA has been linked with cell growth

361   regulation in plants (Arrigoni et al., 1997). Studies with low ascorbate Arabidopsis mutants (*vtc-1*

362   and *vtc2-1*) revealed that these plants had limited growth (Plumb et al., 2018). Thus, aplausible

12

363 hypothesis may be that the rate of AsA synthesis controls the supply of mitochondrial energy for
364 growth.

365 Based on these unanticipated findings, we believe that the wide variability in the synthesis rate of
366 this powerful anti-oxidant molecule in different plant sources, species, during lifecycle and
367 environmental situations might reflect a distinct manner of regulation of plant capacity for
368 adapting their mitochondria to fluctuating energy demands and redox status.

369

370 **MATERIALS AND METHODS**

371 *Plant material*

372 Cherry tomato plants from wild type genotype (*Solanum lycopersicum* 'West Virginia 106') and the
373 tomato P_{35S}:$Slgalldh^{RNAi}$ silenced lines 5 and 8 (Alhagdow et al., 2007) were all grown under
374 standard greenhouse conditions. Tomato fruits were harvested at green-mature stage. For papaya
375 and strawberry, green-mature fruit (*Carica papaya,* 'Golden' cultivar) and red-mature fruit
376 (*Fragaria vesca*, 'Oso Grandi' cultivar) were obtained from local suppliers. When fully-ripe fruits
377 were needed, post-harvest ripening were performed in chambers with controlled temperature
378 (25°C ± 1°C) and relative humidity (85% ± 5%) during nine days. The degree of fruit ripening was
379 assessed by the changes in skin color and pulp firmness (Oliveira et al., 2015).

380 *Mitochondria isolation and purification*

381 Leaf mitochondria were purified following a Percoll density-gradient method as previously
382 described (Keech et al., 2005). Fruit mitochondria were isolated using fruit mesocarp of papaya,
383 tomato and strawberry with defined ripening characteristics, and isolations were performed
384 following general procedures, modified for fruit mitochondria, which were described in (Oliveira et
385 al., 2017).

386 *Respiratory measurements of isolated mitochondria*

387 Immediately after purification, respiration measurement was assessed by O_2 exchange in a Clark
388 electrode (Oxytherm system, Hansatech, UK) using fresh and intact mitochondria (around 20-80
389 µg mitochondrial protein) resuspended in reaction medium (0.35 M mannitol, 10 mM MOPS, 10
390 mM KPO_4, 10 mM KCl, 5 mM $MgCl_2$, and 0.5% (w/v) defatted BSA at pH 7.2 and 25°C). The AOX

391   capacity was assessed by measuring the O_2 consumption rate sensitive to n-propyl gallate

392   (inhibitor of AOX pathway) in the presence of 3 mM of KCN or NaN_3 (Oliveira et al., 2015). The

393   respiratory control rate (RCR) and ADP:O ratio of intact mitochondria were determined using 10

394   mM malate and respiration was calculated as the O_2 uptake rate of the coupled mitochondria in

395   non-phosphorylating state 4, i.e., after consumption of all ADP added in the absence of any

396   inhibitors, as described in previous works (Oliveira et al., 2015). When indicated, mitochondria

397   were energized with distinct respiratory substrates (5 mM L-GalL, 8 mM NADH, 10 mM malate, 20

398   mM glutamate, 5 mM AsA) and oxygen uptake was recorded in presence of AOX and COX

399   inhibitors, salicylhydroxamic acid (SHAM) and NaN_3, respectively. When needed, mitochondria

400   were also treated with 60 µM of CCCP (carbonyl cyanide m-chlorophenyl hydrazone) used as

401   mitochondrial uncoupler of proton gradient (Oliveira et al., 2015).

402   *Measurement of H_2O_2 production by purified mitochondria*

403   The rate of H_2O_2 formation was determined using Amplex Red/horseradish peroxidase (HRP)

404   assay, in a 96-well microplate using a Chameleon Microplate reader (HIDEX), through the

405   detection of the highly fluorescent resorufin, as described previously (Gleason et al., 2011). The

406   concentrations of Amplex Red and HRP in the incubation medium (100 µL final volume per well)

407   were 50 µM and 0.1 U/mL, respectively. The mixture also contained about 10-50 µg of

408   mitochondrial protein prepared in 10 mM MOPS, 10 mM KCl, 5 mM $MgCl_2$ at pH 7.2 and 25°C. For

409   testing respiratory inhibitors/activators, the reaction was supplemented with the defined chemical

410   compounds before adding L-GalL. The chemicals included rotenone (complex I inhibitor),

411   salicylhydroxamic acid, SHAM (AOX inhibitor), pyruvate (AOX activator), antimycin A (complex III

412   inhibitor), diphenylene iodonium, DPI (a flavin-containing oxidase inhibitor) and NaN_3 (complex IV

413   inhibitor). When SHAM was tested, the incubation medium had a higher HRP concentration (0.6

414   U/mL). The reaction was initiated by adding defined L-GalL concentrations into incubation medium

415   and the L-GalL-dependent fluorescence change was recorded with 570 nm excitation and 585 nm

416   emission wavelengths during 15 min. Fluorescence backgrounds of control reactions containing

417   the tested chemicals without L-GalL were allowed to stabilize for two minutes before L-GalL was

418   added to start reaction. To calculate the H_2O_2 level, these backgrounds were subtracted from all

419   fluorescence measured after adding L-GalL. Importantly, as the different compounds used affect

420   the basal fluorescence signal, calibration of all background reactions was done using the same

421   compound concentrations and mitochondrial preparations. The H_2O_2 production was expressed as

422   the corrected change in fluorescence in relation to the corresponding controls.

In vivo detection of ROS formation

424   Mesocarp discs from green-mature papaya fruit were treated with 5 mM L-GalL in 50 mM MOPS

425   buffer pH 7.0 with or without defined respiratory inhibitors that included 2 mM NaN_3, 1 mM

426   SHAM, 20 µM rotenone, 2 µM antimycin A and 5 mM DPI. The treatment of fruit mesocarp with

427   chemicals lasted two hours. Control tissue was subjected to the same procedure without the

428   addition of L-GalL. Afterwards, tissues were incubated in dark for 10 min at 25°C with 500 nM of

429   carboxy-H_2DCFDA (Molecular Probes) and 50 nM of MitoTracker Red CMXRos (Invitrogen).

430   Carboxy-H_2DCFDA permeates membranes and is retained by cells after cleavage of the acetate

431   moiety by cellular esterases and fluorescence develops upon oxidation of the dye by ROS.

432   MitoTracker Red is a membrane potential-sensitive probe that accumulates into mitochondria

433   (Fricker and Meyer, 2001). Stock solutions of the dye were prepared in dimethyl sulfoxide and

434   kept in the dark at −80°C. Before microscopy, samples were quickly rinsed in 50 mM MOPS buffer

435   pH 7.0 to remove any excess of dyes that had not penetrated into the tissue. Microscopy

436   observations were performed using a confocal laser scanning microscope system (Leica TCS SPE

437   laser scanning confocal microscope) using a 63x with 1.4 numerical aperture objective. Carboxy-

438   H_2DCFDA signal was visualized with excitation at 492 nm and emission at 527 nm. MitoTracker Red

439   signal was visualized with excitation at 579 nm and emission at 599 nm. All images were obtained

440   digitally quickly after excitation and all sections observed under the same microscopy parameters

441   by z series stacking. The experiment was repeated twice and led to similar results.

Determination of AsA synthesis capacity in isolated mitochondria and plant tissue

443   Total AsA (reduced and oxidized AsA) was determined as previously described in (Mazorra et al.,

444   2014), with modifications. Briefly, fresh purified mitochondria (10-40 µg) were incubated in 5 mM

445   of L-GalL dissolved in 50 mM TRIS buffer pH 7.8 (in absence of mannitol) for 15, 30, 60 and 120

446   min. When indicated, incubations with L-GalL were performed in presence of respiratory protein

447   inhibitors (rotenone, antimycin A, and DPI) or the AOX activator (pyruvate). For each treatment,

448   corresponding control samples without L-GalL were also included. Reactions were stopped with

449   5% (v/v) trifluoroacetic acid (TFA), centrifuged at 10.000g at 4°C for 10 min, pellet discarded and

450   supernatant neutralized with drops of 100 mM K_2HPO_4 pH 10. Then, samples were reduced with 5

15

451   mM dithiothreitol (DTT) for 5 min, quickly filtrated and finally 20 µL were injected and separated

452   by HPLC (Shimadzu, Kyoto, Japan) using a Spherisorb ODS C-18 column equilibrated with 100 mM

453   phosphate buffer pH 3.0. Runs were performed at 1 mL min^{-1} flux rate at 25 °C. AsA peak was

454   detected at 254 nm with a coupled UV-detector. The AsA synthesis capacity of mitochondria was

455   expressed as the total AsA produced per mitochondrial protein (mg) per time (min). Determination

456   of AsA content in plant tissues was performed as previously described (Bartoli et al., 2006). The

457   AsA synthesis capacity was expressed as total AsA per fresh weight (mg).

458   *Measurement of cytochrome c reduction capacity*

459   The L-GalL-induced Cytc reduction capacity was assessed following procedure described in (Ôba,

460   et al., 1995) with modifications. Purified mitochondria (40-60 µg) were assayed in medium

461   containing 50 mM TRIS buffer pH 7.8, 5% (v/v) Triton X-100, 5 mM Cytc and the reaction was

462   started by adding 5 mM of L-GalL. The formation of reduced cytochrome c was

463   spectrophotometrically monitored at 550 nm every 10 seconds for two minutes. The extinction

464   coefficient of Cytc (21.1 mM^{-1} cm^{-1}) was used for calculating the reaction rate. As indicated,

465   different respiratory inhibitors alone or combined were added into reaction mixture before the

466   start of reaction. The capacity to reduce Cytc was expressed as the amount of Cytc reduced per

467   mitochondria protein per min.

468   *Assessment of changes in FAD redox state*

469   Changes in FAD redox state can be detected based on the fact of FADH$_2$ and FAD are a redox pair

470   but only oxidized FAD is fluorescent and can be monitored without exogenous labeling at 450

471   nm excitation and 520 nm emission wavelengths (Kozioł, 1971). To this, purified mitochondria

472   (20-40 µg) were resuspended in 0.6 mM FAD and 50 mM TRIS buffer pH 7.8 without mannitol. The

473   basal fluorescence was allowed to stabilize during 20 min and then 5 mM L-GalL was added to

474   induce AsA synthesis. The change in fluorescence was recorded every 30 min in both reactions

475   with or without L-GalL. To determine the effects of inhibitors on FAD fluorescence, when

476   indicated, inhibitors were added and the fluorescence backgrounds were recorded. Then, changes

477   in inhibitor-dependent FAD fluorescence in presence of L-GalL were determined. Alterations in

478   FAD redox state were expressed as the difference between fluorescence (final minus initial) values

479   within 30 minute intervals.

16

480   *Measurement of ubiquinol production capacity*

481   To assess the ability of L-GalL to convert ubiquinone into ubiquinol, purified mitochondria (40-60

482   µg) were incubated with 5 mM of L-GalL, 15 µM of ubiquinone (UQ10) in 1 mL of 50 mM TRIS

483   buffer pH 7.8 for 4 h in dark. Incubations were done in the presence of 3 mM NaN_3, 1 mM SHAM

484   to avoid ubiquinol re-oxidation. Controls without L-GalL were also included. Extractions were

485   performed based on procedure published by (Wagner and Wagner, 1995) with modifications.

486   Briefly, reactions were stopped with 10 % (v/v) TFA, extracted in shade with 600 µL of cold-

487   hexane, vortexed for 1 min, centrifuged at 6.000g at 4°C for 5 min. Then, the upper hexane phase

488   was collected, evaporated to dryness in a rapidVap evaporation system and finally the extracted

489   UQH_2/UQ was re-suspended in 500 µL of acetone. Samples were filtrated to analyze in HPLC. 20 µL

490   were injected in reverse-phase C-18 column equilibrated with acetonitrile:etanol 3:1 (v/v). Runs

491   were done at 1.5 mL min^{-1} flux rate and 40°C. The ubiquinol ($UQH_2$10) peak was detected with a

492   fluorescence detector at 290 nm (exc), 370 nm (em), as described in Yoshida et al. (2010). The

493   ubiquinone reduction capacity was expressed as the ubiquinol/ubiquinone ratio determined after

494   incubation in the presence of L-GalL over 4 hours.

495   *Assessment of NADH production capacity by isolated mitochondria*

496   The NADH production was based on the difference in the absorption spectra of NAD^+ and NADH.

497   The NADH shows absorption maxima at 340 nm but NAD^+ does not absorb light at 340 nm

498   (Renault et al., 1982). In brief, mitochondria were osmotically-broken by incubating into 10 mM

499   MOPS (without mannitol) pH 7.2, 0.1 mM EDTA during 10 min. Then, a reaction mixture was

500   prepared consisting of 5 mM L-GalL, 20 mM NAD^+, 3 mM azyde and 1 mM SHAM, allowed to react

501   during 30 min at 25°C and NADH absorbance (extinction coefficient NADH = 6.220 M^{-1} cm^{-1}) was

502   read with UV/Vis spectrophotometer. Control mixture had the same components, except L-GalL.

503   The relative NADH production was determined as the difference in absorbance at 340 nm

504   following incubation for 30 min.

505   *Measurement of H^+-ATPase pumping activity*

506   The H^+-ATPase activity was measured using sub-mitochondrial particles obtained from intact

507   mitochondria treated or not with L-GalL. Particles were prepared by sonication, as described in

508   (Ragan et al., 1987), with some modifications. Briefly, intact mitochondria (200 µg) were incubated

509   in 10 mM MOPS containing 0.35 M mannitol with or without 5 mM L-GalL over 60 min at 25°C.

510   Following treatment, mitochondria were sonicated by 6-10 s pulses with 30 s intervals and

511   supernatant ultra-centrifuged and the resulting pellet (sub-mitochondrial particles) were re-

512   suspended into the same buffer. Then, sonicated-disrupted mitochondria solution was incubated

513   with 1 mM ATP and its capacity to hydrolyze ATP was monitored by measuring the release of

514   inorganic phosphate (P_i) colorimetrically at 720 nm, as previously reported in (Subbarow, 1925).

515   H^+-ATPase activity was expressed as the amount of released Pi during 1 min into the reaction

516   medium.

517   *Measurement of ATP level*

518   To determine the mitochondrial capacity to synthesize ATP during ascorbate biosynthesis, 50 μg of

519   freshly purified intact mitochondria were incubated in medium containing 10 mM MOPS, 150 mM

520   sucrose, 7.5 mM KCl, 5 mM $MgCl_2$, 7.5 mM KPi and 5 mM of L-GalL during 10 min. Then, reaction

521   was initiated adding 10 mM malate and 50 μM of ADP and allowed to incubate at 25°C during 30

522   min. Control reactions were run in absence of ADP and malate. Mitochondrial ATP was extracted

523   by boiling the samples for 15 min. After centrifugation at 9000g for 15 min, ATP content in 200 μL

524   of supernatants was determined by the bioluminescent assay based on luciferin-luciferase method

525   (Sigma-Aldrich, FLAA) using a luminescence spectrophotometer (RF5301PC, Shimadzu) at 560 nm

526   of emission wavelength. The reaction was initiated by addition of 20 μL of ATP assay mix (Sigma-

527   Aldrich, FLAAM) in a mixture containing 1800 μL of ATP assay buffer (10 mM $MgSO_4$, 1 mM DTT, 1

528   mM EDTA, 100 μg.mL^{-1} bovine serum albumin, and 50 mM tricine buffer salts, pH 7.8) and 200 μL

529   of sample. The reaction was monitored for 1 min. Calibration curve was performed previously in

530   the same conditions with ATP standard solutions ranging from 0.1 to 10 μmol.

531   To determine ATP content in plants, 600-900 mg of aboveground plant tissue were collected at

532   night-time (two hours before lighting) and were quickly incubated at 100°C for 15 min in 1 mL of

533   boiled water, as described in (Yamamoto et al., 2002). Tissues were homogenized at 4°C and then

534   centrifuged at 9000g for 15 min at 4°C. Supernatant (200 μL) was used for ATP quantification, as

535   described above.

536   *Western blot analysis*

18

537   Mitochondrial proteins were reduced using 2.5% (v/v) 2-mercaptoethanol into sample buffer,

538   loaded onto one-dimensional SDS/PAGE gels and run following standard procedures. For the

539   detection of oxidized AOX, mitochondrial proteins were prepared in absence of 2-

540   mercaptoethanol. Molecular weight markers (24-102 kDa, GE Healthcare) were used and equal

541   loading of gels (25 µg protein) was checked by Ponceau staining. The proteins were transferred to

542   a nitrocellulose membrane (Hybond ECL, Amersham/GE Healthcare); the membrane was blocked

543   in nonfat milk 5% overnight at 4°C and antibodies against L-GalLDH and AOX (commercially

544   provided by Agrisera) were used in dilutions 1:500. Then, the membranes were washed three

545   times in PBS buffer with milk 5%, incubated with goat anti-rabbit secondary antibody for 2h, and

546   subsequently washed in PBS buffer three times. Results were visualized by chemiluminiscence

547   with a ECL Western Blotting Detection System (Amersham/GE Healthcare) and quantified using

548   ImageJ densitometric software (https://imagej.nih.gov/ij/).

549   *Experimental design for comparative proteomic analysis*

550   Papaya fruit mesorcarp discs (500 mg fresh weight) were treated with 5 mM of L-GalL, 50 mM

551   MOPS buffer pH 7.0 for two hours at 25°C. A control sample without L-GalL was also incubated

552   under the same conditions. Then, three independent samples of proteins were extracted from

553   each treatment. Procedures for protein extraction, digestion and mass spectrometry analysis are

554   performed following previous works described in (Heringer et al., 2017).

555   *Bioinformatic analysis*

556   Progenesis QI for Proteomics Software V.2.0 (Nonlinear Dynamics, Newcastle, UK) were used to

557   spectra processing and database searching conditions. The analysis were performed using

558   following parameters: Apex3D of 150 counts for low energy threshold, 50 counts for elevated

559   energy threshold, and 750 counts for intensity threshold; one missed cleavage, minimum fragment

560   ion per peptide equal to two, minimum fragment ion per protein equal to five, minimum peptide

561   per protein equal to two, fixed modifications of carbamidomethyl (C) and variable modifications of

562   oxidation (M) and phosphoryl (STY), and a default false discovery rate (FDR) value at a 4%

563   maximum, peptide score greater than four, and maximum mass errors of 10 ppm. The analysis

564   used the *Carica papaya* v. 0.4 protein databank from Phytozome (https://phytozome.jgi.doe.gov/).

565   Label-free relative quantitative analyses were performed based on the ratio of protein ion counts

19

566   among contrasting samples. After data processing and to ensure the quality of results, only

567   proteins present in 3 of 3 runs were accepted. Furthermore, differentially abundant proteins were

568   selected based on a fold change of at least 1.5 and ANOVA ($P \leq 0.05$). Functional annotation was

569   performed using Blast2Go software v. 3.4 (Conesa et al., 2005).

570   *Seed treatment, plant growth and photosynthesis*

571   To determine growth of tomato plants with induced AsA synthesis, seeds of wild type and L-

572   GalLDH-RNAi plant lines were subjected to imbibition treatment with 20 mM GalL for 6 hours. In

573   parallel, control seeds were treated in absence of L-GalL. Imbibited seeds were sown on soil pots

574   filled with commercial substrate and irrigated with Hoagland solution. Then, seedlings (one per

575   pot) were grown for four weeks at a growth chamber at 25°C with a 16-h photoperiod at a light

576   intensity of 500 μmol m^2 s^{-1}. Height and biomass of plants were determined at given time points.

577   Dry weights were determined by drying aboveground tissue in an air circulation oven at 80°C for

578   one week. Height was determined by measuring the distance from the ground to the top of

579   canopy. At four-weeks after sowing, instantaneous gas exchange measurements were done on six

580   recently fully expanded leaves in the upper part of the wild type plant and L-GalLDH-RNAi plant

581   lines. Measurements were taken between 2-4 hours after the start of light period using a gas

582   exchange system (LiCOR, Biosciences, Lincoln, NE, USA). Determinations of CO_2 assimilation were

583   performed at light intensity 500 $\mu mol m^{-2} s^{-1}$, 400 ppm CO_2 and temperature 24-26°C.

584   *Statistical analysis*

585   Data from at least three independent biochemical experiments were averaged and subjected to

586   ANOVA and, when needed, means were analyzed following Tukey test at $P \leq 0.05$.

587

588   **ACKNOWLEDGEMENTS**

594 were granted with a CAPES-DSc; S.F.P. was granted with a CNPq-DSc, and T.R.O. and R.S.R. were

595 granted with a FAPERJ-DSc. fellowship.

596

597 **_TABLES_**

598 **Table I.** Effect of L-GalL on the mitochondrial ability to perform electron transport and coupled

599 ATP synthesis.

	Treatments	
	Control	**+ 5mM GalL**
Phosphorylation efficiency[*]	3.06±0.15	0.63±0.16
Coupling efficiency	2.93±0.17	1.61±0.14
Depolarization	119%	0%
NADH production	0.021±0.0081	0.240±0.1731
H^+-ATPase activity	208.07±29.87	365.46±78.74
UQH_2/UQ ratio	2.49±0.81	7.05±0.24
ATP synthesis capacity	0.0373±0.0012	0.0298±0.0021

600 [*]Efficiency of phosphorylation and coupling were determined recording the O_2 uptake rate of the coupled
601 mitochondria in non-phosphorylating and phosphorylating states and expressed as ADP:O ratio and the
602 respiratory control rate (RCR), respectively. Membrane depolarization was assessed by measuring the
603 percentage of increase in the oxygen uptake induced by a respiratory uncoupler. Mitochondrial potential to
604 reverse the electron flux was determined by quantifying the capacities to convert exogenous NAD^+ into
605 NADH and to hydrolyze ATP in ADP and Pi. The capacity to alter the ubiquinone redox state was measured
606 by the conversion of exogenously added oxidized ubiquinone into its reduced form and expressed as the
607 ubiquinol/ubiquinone ratio. ATP synthesis capacity was assessed by quantifying the increase in the synthesis
608 of ATP after adding ADP. All values are means± standard error from three independent mitochondrial
609 preparations.

610

611

612

613   **Table II.** Summary of proteins differentially regulated by L-GalL in papaya fruit mesocarp.

Identification number	Blast2GO description	Fold change L-GalL/Control
Up-regulated proteins[*]		
pacid=16406756	40S ribosomal S8	7.2
pacid=16407487	pyruvate kinase cytosolic-like isoform X1	7.1
pacid=16427581	probable thimet oligopeptidase isoform X3	3.5
pacid=16431084	SEC14 cytosolic factor family phosphoglyceride transfer family isoform 2	2.6
pacid=16404296	40S ribosomal S2-2-like	2.3
pacid=16425273	glycerophosphodiester phosphodiesterase chloroplastic-like	2.3
pacid=16421901	Hydroxyproline-rich glyco family isoform 2	2.1
pacid=16423413	60S ribosomal L8-3	2.1
pacid=16408435	plasma membrane ATPase 4 isoform X1	2.1
pacid=16423505	Phospholipase D delta	2.1
pacid=16415693	clathrin light chain 1-like	2.0
pacid=16407929	sirohydrochlorin chloroplastic-like	2.0
pacid=16409797	transport SEC23-like	1.9
pacid=16409547	probable thiol methyltransferase 2 isoform X3	1.9
pacid=16404282	60S ribosomal L23A	1.8
pacid=16415376	NADH dehydrogenase subunit 7 (mitochondrion)	1.8
pacid=16421330	ferritin- chloroplastic-like	1.7
pacid=16410499	argonaute 1	1.7
pacid=16417105	probable low-specificity L-threonine aldolase 1	1.6
pacid=16422730	cell division cycle 48 homolog	1.6
pacid=16426064	probable glutathione S-transferase	1.6
pacid=16423032	40S ribosomal S3a	1.6
pacid=16405013	GATA zinc finger domain-containing isoform 1	1.5

pacid=16407528	phosphoenolpyruvate carboxykinase [ATP]	1.5
Down-regulated proteins		
pacid=16422946	cysteine synthase	0.7
pacid=16429847	L-ascorbate peroxidase cytosolic	0.7
pacid=16426651	Succinate dehydrogenase 5	0.7
pacid=16406290	probable fructokinase- chloroplastic	0.6
pacid=16415704	alpha-galactosidase family	0.6
pacid=16417606	nascent polypeptide-associated complex subunit alpha 1	0.6
pacid=16431407	thioredoxin-dependent peroxidase	0.6
pacid=16427996	probable polygalacturonase isoform X3	0.6
pacid=16413137	cysteine ase RD21A-like	0.6
pacid=16426375	glyoxylate succinic semialdehyde reductase 1	0.6
pacid=16413886	nucleoside diphosphate kinase B	0.6
pacid=16406032	leucine--tRNA cytoplasmic	0.6
pacid=16428645	14 kDa zinc-binding	0.6
pacid=16414991	E3 ubiquitin- ligase RNF25	0.5
pacid=16406747	NAD(P)H dehydrogenase (quinone) FQR1	0.5
pacid=16412645	26S protease regulatory subunit 6B homolog	0.5
pacid=16418146	PREDICTED: uncharacterized protein LOC105784633	0.5
pacid=16411412	GTP-binding SAR1A	0.5
pacid=16420462	heat shock 70 kDa	0.5
pacid=16413904	GTP-binding YPTM2	0.4
pacid=16414185	3-hydroxyisobutyryl- hydrolase mitochondrial isoform X1	0.4
pacid=16422671	MLP 43	0.4
pacid=16405578	alpha-1,4-glucan- synthase [UDP-forming] 2	0.4
pacid=16425822	cysteine ase inhibitor 5	0.4
pacid=16424442	cell division cycle 48 homolog	0.2
pacid=16426123	trehalose-6-phosphate synthase	0.1

| pacid=16430375 | dirigent 22-like | 0.06 |
| pacid=16425257 | 10 kDa chaperonin-like | 0.05 |

614 * Up-regulated and down-regulated proteins represent those having a fold change of at least 1.5 (ANOVA,
615 p<0.05) relative to the treatment without L-GalL (control). As criteria for reproducibility, only proteins
616 identified with differential abundance were included in the table. The bioinformatic analysis used the *Carica*
617 *papaya* v. 0.4 protein databank from Phytozome and the functional annotation was done using Blast2Go
618 software v.3.4.

619

620

621 ***FIGURE CAPTIONS***

622 **Figure 1A**. NADH-driven respiration of leaf mitochondria purified from 30-days-old wild type, 8-14

623 and 5-13 transgenic lines. Mitochondrial preparations were pre-treated or not with 5 mM L-GalL

624 and the oxygen uptake rates were determined following the addition of 10 mM malate. Then, the

625 respiration was blocked by a mixture of respiratory inhibitors 5 mM SHAM and 3 mM NaN3. **1B**.

626 Immunoblot of L-GalLDH in leaf mitochondria from 30-days-old wild type, 8-14 and 5-13

627 transgenic lines detected by Western Blot using anti-L-GalLDH (Agrisera). Relative abundance,

628 expressed as % of wild type signal, was obtained by densitometry. L-GalLDH activity (measured as

629 rate of Cytc reduction) was determined in the mitochondria from 30-days-old wild type, 8-14 and

630 5-13 transgenic lines. Values represent means ± standard error and asterisks represent significant

631 differences between inhibited and non-inhibited reactions analyzed by one-way ANOVA following

632 by Tukey test (P < 0.05). Measurements from three independent mitochondrial preparations (n=3).

633 **1C**. Rates of oxygen uptake SHAM-sensitive and NaN3-resistant (alternative respiration)

634 determined in mitochondria from wild type, 8-14 and 5-13 transgenic lines. Asterisks represent

635 significant differences of alternative respiration of transgenic leaf mitochondria when compared to

636 wild type by one-way ANOVA following by Tukey test (P < 0.05). **1D**. Immunoblot of AOX detected

637 when mitochondrial proteins are loaded without the reducing agent of free sulphydryl residues (2-

638 mercaptoethanol) into sample buffer. A 66 kDa protein was detected by Western Blot using anti-

639 AOX antibodies (Agrisera) in leaf mitochondria purified from 30-days-old wild type, 8-14 and 5-13

640 plants. Immunoblot of AOX (molecular weight of about 33 kDa) obtained when the reducing agent

641 was added into sample buffer and subsequent detection with anti-AOX antibodies. Equal loading

642 of gels was checked by Ponceau staining. Relative abundances were assessed by quantification of

643 signals through densitometry and expressed as % of wild type level.

644   **Figure 2A**. Ascorbate production capacity measured in pure mitochondria treated or not with

645   inhibitors (3 mM azyde, NaN3, 1mM SHAM, 2 µM antimycin A, 20 µM rotenone, and 5 mM DPI).

646   Ascorbate synthesis was initiated in presence of 5 mM L-GalL. **2B**. Activity of L-GalLDH enzyme

647   (assessed as capacity to reduce Cytc) determined in purified mitochondria incubated with 1mM

648   SHAM, 2 µM antimycin A, 20 µM rotenone, and 5 mM DPI). Cytc reduction was started by adding

649   5mM L-GalL in presence of the Cytc oxidase inhibitor, azyde. **2C**. Ascorbate production and L-

650   GalLDH activity determined in mitochondria from green-mature and full-ripe papaya fruit. **2D**.

651   Ascorbate synthesis-dependent changes in flavin adenine dinucleotide (FAD) fluorescence

652   measured in pure mitochondria incubated with the inhibitor compounds indicated above in figure

653   2A. AsA synthesis was started with 5mM L-GalL. Bars represent means ± standard error from at

654   least three independent experiments.

655   **Figure 3A**. Induction of hydrogen peroxide (H2O2) production by 5 mM L-GalL in pure

656   mitochondria treated with 1 mM SHAM, 3 mM azyde, 20 µM rotenone, 2 µM antimycin A, and 5

657   mM DPI. H2O2 content was quantified using Amplex Red/horseradish peroxidase (HRP) assay and

658   relative H2O2 level for all treatments was normalized to their corresponding controls without L-

659   GalL. Bars are means ± standard error (n=3). **3B**. Representative confocal images of co-localization

660   of ROS and mitochondria stains in fruit mesocarp tissue incubated with 5 mM L-GalL and the same

661   inhibitor compounds as above. Mitochondria were localized with Mito-Tracker Red and ROS

662   detection was performed with (2,7-dichlorodihydrofluorescein diacetate, DCF-DA). Scale bar 10

663   µm.

664   **Figure 4A**. Ascorbate synthesis capacity and ATP content of leaf tissue (in dark) determined in leaf

665   tissue from four weeks-days-old wild type, 8-14 and 5-13 transgenic lines. **4B**. Effect of seed

666   treatment with 20mM L-GalL on seedling growth from wild type, 8-14 and 5-13 transgenic lines

667   measured one-week and four-weeks following the chemical treatment. **4C**. Net photosynthesis of

668   fully expanded leaves (Dotted line) and dry weight of aboveground tissue (Grey line) determined

669   in wild type, 8-14 and 5-13 transgenic lines at the four-weeks growth stage. All bars are means ±

670   standard error from three independent experiments.

671

672   ***REFERENCES***

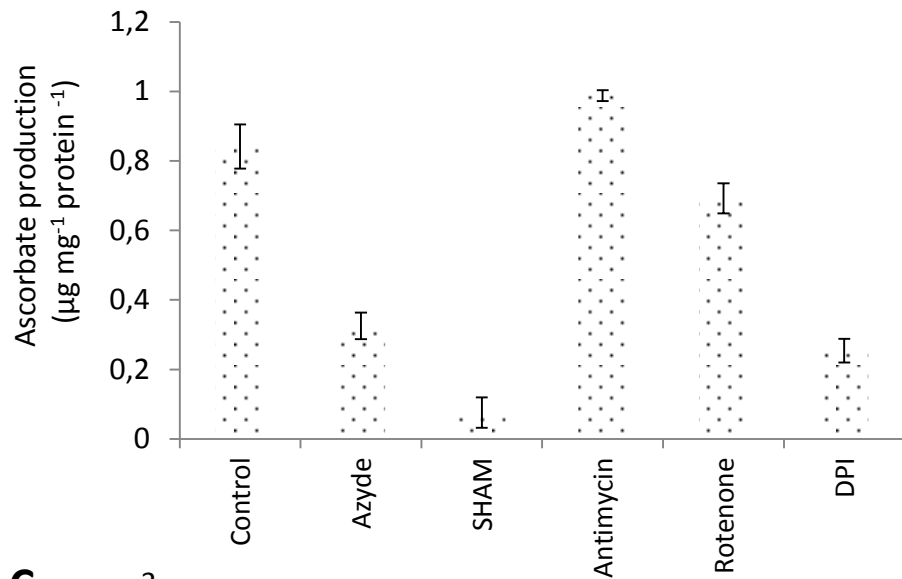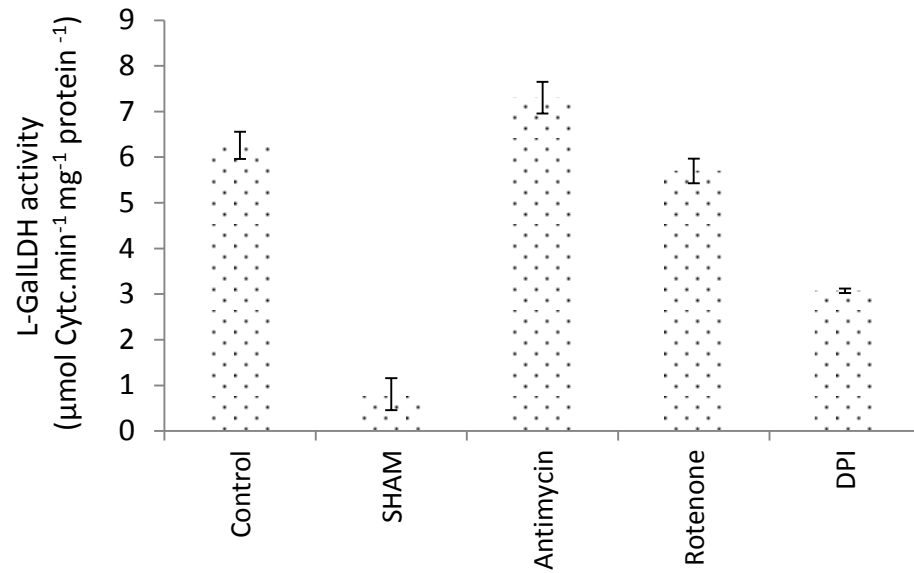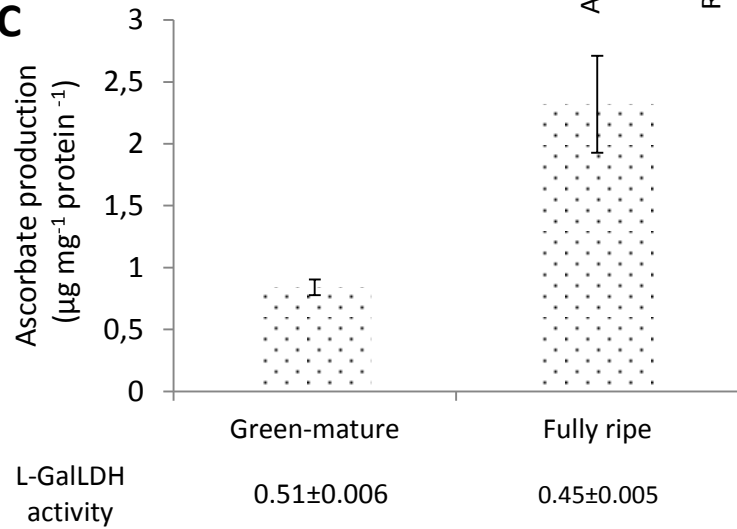673   **Alhagdow M, Mounet F, Gilbert L, Nunes-Nesi A, Garcia V, Just D, Petit J, Beauvoit B, Fernie AR,**
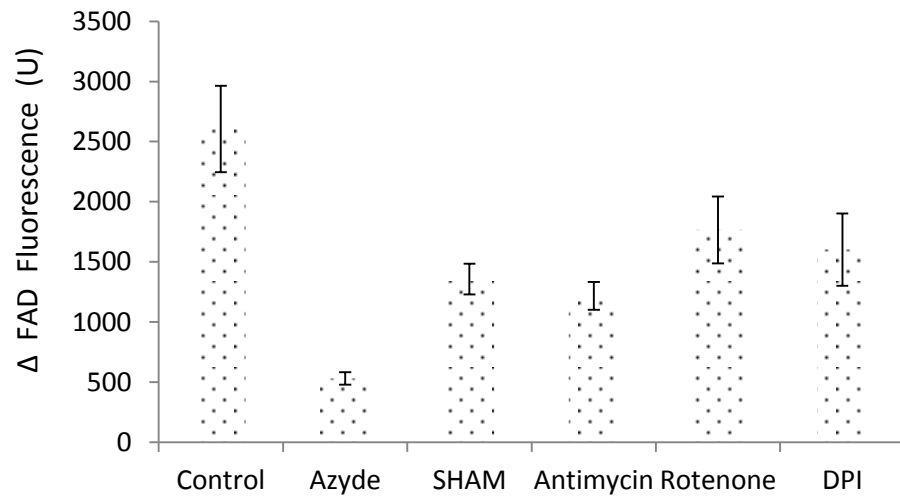
674 **Rothan C, et al** (2007) Silencing of the Mitochondrial Ascorbate Synthesizing Enzyme L-
675 Galactono-1,4-Lactone Dehydrogenase Affects Plant and Fruit Development in Tomato. Plant
676 Physiol **145**: 1408–1422

677 **Arrigoni O, Calabrese G, De Gara L, Bitonti MB, Liso R** (1997) Correlation between changes in cell
678 ascorbate and growth of Lupinus albus seedlings. J Plant Physiol **150**: 302–308

679 **Bartoli CG, Pastori GM, Foyer CH** (2000) Ascorbate biosynthesis in mitochondria is linked to the
680 electron transport chain between complexes III and IV. Plant Physiol **123**: 335–44

681 **Bartoli CG, Yu J, Gómez F, Fernández L, McIntosh L, Foyer CH** (2006) Inter-relationships between
682 light and respiration in the control of ascorbic acid synthesis and accumulation in Arabidopsis
683 thaliana leaves. J Exp Bot **57**: 1621–1631

684 **Conesa A, Götz S, García-Gómez JM, Terol J, Talón M, Robles M** (2005) Blast2GO: a universal tool
685 for annotation, visualization and analysis in functional genomics research. Bioinforma Appl
686 NOTE **21**: 3674–3676

687 **Dahal K, Vanlerberghe GC** (2017) Alternative oxidase respiration maintains both mitochondrial
688 and chloroplast function during drought. New Phytol **213**: 560–571

689 **Davletova S, Rizhsky L, Liang H, Shengqiang Z, Oliver DJ, Coutu J, Shulaev V, Schlauch K, Mittler R**
690 (2005) Cytosolic ascorbate peroxidase 1 is a central component of the reactive oxygen gene
691 network of Arabidopsis. Plant Cell **17**: 268–81

692 **Foyer CH, Kiddle G, Verrier P** (2007) Transcriptional profiling approaches to understanding how
693 plants regulate growth and defence: A case study illustrated by analysis of the role of vitamin
694 C. Plant Syst. Biol. Birkhäuser Basel, Basel, pp 55–86

695 **Fricker MD, Meyer AJ** (2001) Confocal imaging of metabolism in vivo: pitfalls and possibilities. J
696 Exp Bot **52**: 631–640

697 **Gleason C, Huang S, Thatcher LF, Foley RC, Anderson CR, Carroll AJ, Millar AH, Singh KB** (2011)
698 Mitochondrial complex II has a key role in mitochondrial-derived reactive oxygen species
699 influence on plant stress gene regulation and defense. Proc Natl Acad Sci U S A **108**: 10768–
700 73

701 **Grillet L, Ouerdane L, Flis P, Hoang MTT, Isaure M-P, Lobinski R, Curie C, Mari S** (2014) Ascorbate
702 efflux as a new strategy for iron reduction and transport in plants. J Biol Chem **289**: 2515–25

703 **Hao H-X, Khalimonchuk O, Schraders M, Dephoure N, Bayley J-P, Kunst H, Devilee P, Cremers**
704 **CWRJ, Schiffman JD, Bentz BG, et al** (2009) SDH5, a gene required for flavination of succinate
705 dehydrogenase, is mutated in paraganglioma. Science **325**: 1139–42

706 **Heringer AS, Reis RS, Passamani LZ, de Souza-Filho GA, Santa-Catarina C, Silveira V** (2017)
707 Comparative proteomics analysis of the effect of combined red and blue lights on sugarcane
708 somatic embryogenesis. Acta Physiol Plant **39**: 52

709 **Holtzapffel RC, Finnegan PM, Millar AH, Badger MR, Day DA** (2002) Mitochondrial protein
710 expression in tomato fruit during on-vine ripening and cold storage. Funct Plant Biol **29**: 827

711 **Huang S, Millar AH** (2013) Succinate dehydrogenase: the complex roles of a simple enzyme. Curr
712 Opin Plant Biol **16**: 344–349

713 **Keech O, Dizengremel P, Gardeström P** (2005) Preparation of leaf mitochondria from *Arabidopsis*
714 *thaliana*. Physiol Plant **124**: 403–409

715 **Kotchoni SO, Larrimore KE, Mukherjee M, Kempinski CF, Barth C** (2009) Alterations in the
716 endogenous ascorbic acid content affect flowering time in Arabidopsis. Plant Physiol **149**:
717 803–815

718 **Kozioł J** (1971) [132] Fluorometric analyses of riboflavin and its coenzymes. Methods Enzymol **18**:
719 253–285

720 **Kühn K, Yin G, Duncan O, Law SR, Kubiszewski-Jakubiak S, Kaur P, Meyer E, Wang Y, Small CC des**
721 **F, Giraud E, et al** (2015) Decreasing electron flux through the cytochrome and/or alternative

722   respiratory pathways triggers common and distinct cellular responses dependent on growth
723   conditions. Plant Physiol **167**: 228–50

724 **Leferink NGH, Donald M, Jose F, Van Den Berg WAM, Van Berkel WJH** (2009) Functional
725   assignment of Glu386 and Arg388 in the active site of L-galactono-c-lactone dehydrogenase.
726   FEBS Lett **583**: 3199–3203

727 **Mailloux RJ, Harper M-E** (2011) Uncoupling proteins and the control of mitochondrial reactive
728   oxygen species production. Free Radic Biol Med **51**: 1106–1115

729 **Mazorra LM, Senn ME, Grozeff GEG, Fanello DD, Carrión CA, Núñez M, Bishop GJ, Bartoli CG**
730   (2014) Impact of brassinosteroids and ethylene on ascorbic acid accumulation in tomato
731   leaves. Plant Physiol Biochem **74**: 315–322

732 **Millar AH, Whelan J, Soole KL, Day DA** (2011) Organization and Regulation of Mitochondrial
733   Respiration in Plants. Annu Rev Plant Biol **62**: 79–104

734 **Mukherjee M, Larrimore KE, Ahmed NJ, Bedick TS, Barghouthi NT, Traw MB, Barth C** (2010)
735   Ascorbic Acid Deficiency in *Arabidopsis* Induces Constitutive Priming That is Dependent on
736   Hydrogen Peroxide, Salicylic Acid, and the *NPR1* Gene. Mol Plant-Microbe Interact **23**: 340–
737   351

738 **Noctor G, Foyer CH** (2016) Intracellular Redox Compartmentation and ROS-Related
739   Communication in Regulation and Signaling. Plant Physiol **171**: 1581–92

740 **Noctor G, De Paepe R, Foyer CH** (2007) Mitochondrial redox biology and homeostasis in plants.
741   Trends Plant Sci **12**: 125–134

742 **Nunes-Nesi A, Araújo WL, Fernie AR** (2011) Targeting mitochondrial metabolism and machinery as
743   a means to enhance photosynthesis. Plant Physiol **155**: 101–107

744 **Ôba, K, Ishikawa S, Nishikawa M, Mizuno H, Yamamoto T** (1995) Purification and Properties of L-
745   Galactono- γ-Lactone Dehydrogenase, a Key Enzyme for Ascorbic Acid Biosynthesis, from
746   Sweet Potato Roots. J Biochem **117**: 120–124

747 **Oliveira JG, Mazorra LM, Silva GMC, da Cruz Saraiva KD, Santana DB, dos Santos CP, Oliveira MG,**
748   **Costa JH** (2017) Procedures of Mitochondria Purification and Gene Expression to Study
749   Alternative Respiratory and Uncoupling Pathways in Fruits. Plant Respir. Intern. Oxyg.
750   Humana Press, New York, NY, pp 143–165

751 **Oliveira MG, Mazorra LM, Souza AF, Silva GMC, Correa SF, Santos WC, Saraiva KDC, Teixeira AJ,**
752   **Melo DF, Silva MG, et al** (2015) Physiology Involvement of AOX and UCP pathways in the
753   post-harvest ripening of papaya fruits. J Plant Physiol **189**: 42–50

754 **Pineau B, Mathieu C, Gérard-Hirne C, De Paepe R, Chétrit P** (2005) Targeting the NAD7 subunit to
755   mitochondria restores a functional complex I and a wild type phenotype in the Nicotiana
756   sylvestris CMS II mutant lacking nad7. J Biol Chem **280**: 25994–26001

757 **Plumb W, Townsend AJ, Rasool B, Alomrani S, Razak N, Karpinska B, Ruban A V, Foyer CH** (2018)
758   Ascorbate-mediated regulation of growth, photoprotection, and photoinhibition in
759   Arabidopsis thaliana. J Exp Bot **69**: 2823–2835

760 **Ragan CI, Wilson MT, Darley-Usmar VM LP** (1987) Sub-fractionation of mitochondria and isolation
761   of the proteins of oxidative phosphorylation. IRL Press

762 **Renault G, Raynal E, Sinet M, Berthier JP, Godard B, Cornillault J** (1982) A laser fluorimeter for
763   direct cardiac metabolism investigation. Opt Laser Technol **14**: 143–148

764 **Schertl P, Braun H-P** (2014) Respiratory electron transfer pathways in plant mitochondria. Front
765   Plant Sci **5**: 163

766 **Schertl P, Sunderhaus S, Klodmann J, Grozeff GEG, Bartoli CG, Braun H-P** (2012) L-galactono-1,4-
767   lactone dehydrogenase (GLDH) forms part of three subcomplexes of mitochondrial complex I
768   in Arabidopsis thaliana. J Biol Chem **287**: 14412–9

769 **Schluepmann H, Pellny T, Dijken A van, Smeekens S, Paul M** (2003) Trehalose 6-phosphate is

770   indispensable for carbohydrate utilization and growth in Arabidopsis thaliana. Proc Natl Acad
771   Sci **100**: 6849–6854

772   **Selinski J, Hartmann A, Deckers-Hebestreit G, Day DA, Whelan J, Scheibe R** (2018) Alternative
773   Oxidase Isoforms Are Differentially Activated by Tricarboxylic Acid Cycle Intermediates. Plant
774   Physiol **176**: 1423–1432

775   **Smirnoff N** (2018) Ascorbic acid metabolism and functions: A comparison of plants and mammals.
776   Free Radic Biol Med **122**: 116–129

777   **Smirnoff N** (2011) Vitamin C: The Metabolism and Functions of Ascorbic Acid in Plants. Adv Bot
778   Res **59**: 107–177

779   **Subbarow CHF and Y** (1925) The colorimetric determination of phosphorus. J Chem Inf Model **6**:
780   375–400

781   **Sweetlove LJ, Beard KFM, Nunes-Nesi A, Fernie AR, Ratcliffe RG** (2010) Not just a circle: Flux
782   modes in the plant TCA cycle. Trends Plant Sci **15**: 462–470

783   **Tamaoki M, Mukai F, Asai N, Nakajima N, Kubo A, Aono M, Saji H** (2003) Light-controlled
784   expression of a gene encoding l-galactono-γ-lactone dehydrogenase which affects ascorbate
785   pool size in Arabidopsis thaliana. Plant Sci **164**: 1111–1117

786   **Umbach AL, Ng VS, Siedow JN** (2006) Regulation of plant alternative oxidase activity: A tale of two
787   cysteines. doi: 10.1016/j.bbabio.2005.12.005

788   **Vanlerberghe GC** (2013) Alternative Oxidase: A Mitochondrial Respiratory Pathway to Maintain
789   Metabolic and Signaling Homeostasis during Abiotic and Biotic Stress in Plants. Int J Mol Sci
790   **14**: 6805–6847

791   **Vanlerberghe GC, Martyn GD, Dahal K** (2016) Alternative oxidase: a respiratory electron transport
792   chain pathway essential for maintaining photosynthetic performance during drought stress.
793   Physiol Plant **157**: 322–337

794   **Wagner AM, Wagner MJ** (1995) Measurements of in Vivo Ubiquinone Reduction Levels in Plant
795   Cells. Plant Physiol **108**: 277–283

796   **Westlake TJ, Ricci WA, Popescu G V, Popescu SC** (2015) Dimerization and thiol sensitivity of the
797   salicylic acid binding thimet oligopeptidases TOP1 and TOP2 define their functions in redox-
798   sensitive cellular pathways. Front Plant Sci **6**: 327

799   **Yamamoto Y, Kobayashi Y, Devi SR, Rikiishi S, Matsumoto H** (2002) Aluminum toxicity is
800   associated with mitochondrial dysfunction and the production of reactive oxygen species in
801   plant cells. Plant Physiol **128**: 63–72

802   **Yoshida K, Shibata M, Terashima I, Noguchi K** (2010) Simultaneous Determination of In Vivo
803   Plastoquinone and Ubiquinone Redox States by HPLC-Based Analysis. Plant Cell Physiol **51**:
804   836–841

805   **Yuan L-B, Dai Y-S, Xie L-J, Yu L-J, Zhou Y, Lai Y-X, Yang Y-C, Xu L, Chen Q-F, Xiao S** (2017)
806   Jasmonate Regulates Plant Responses to Postsubmergence Reoxygenation through
807   Transcriptional Activation of Antioxidant Synthesis. Plant Physiol **173**: 1864–1880

808
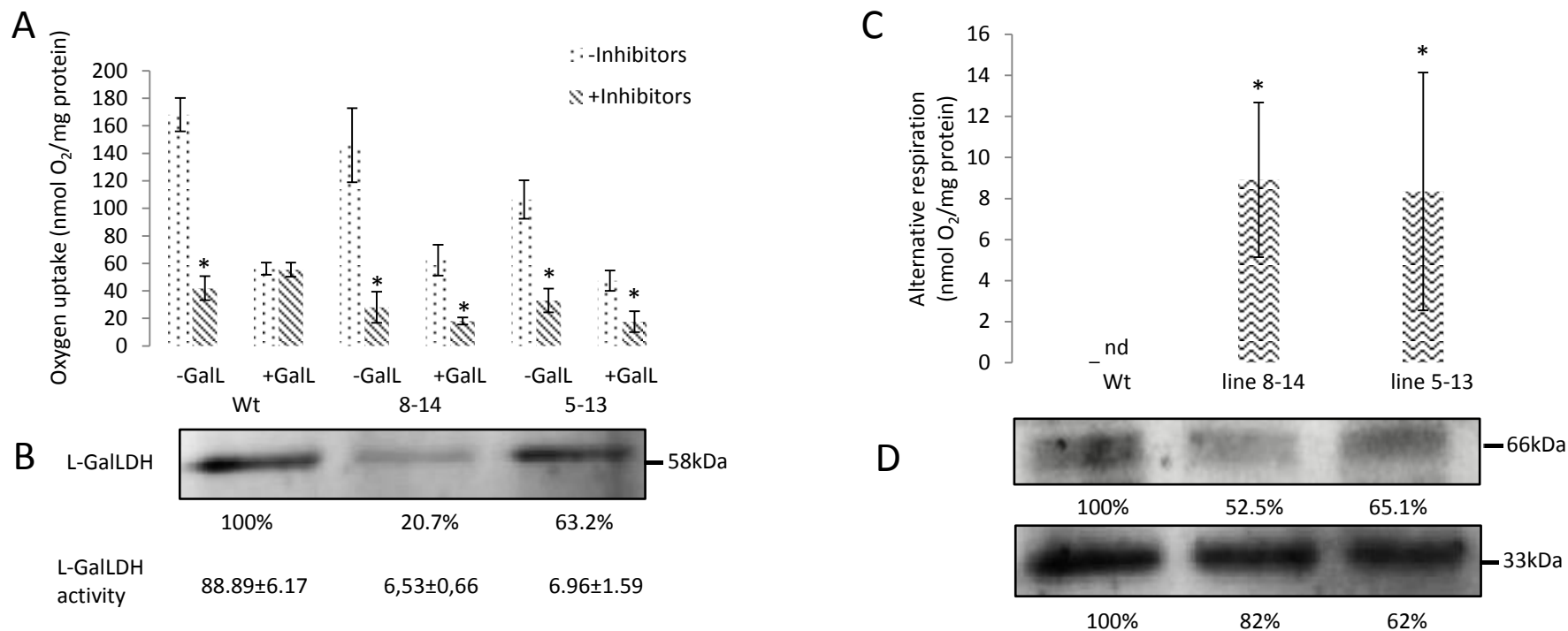
Figure 1A. NADH-driven respiration of leaf mitochondria purified from 30-days-old wild type, 8-14 and 5-13 transgenic lines. Mitochondrial preparations were pre-treated or not with 5 mM L-GalL and the oxygen uptake rates were determined following the addition of 10 mM malate. Then, the respiration was blocked by a mixture of respiratory inhibitors 5 mM SHAM and 3 mM NaN3. **1B**. Immunoblot of L-GalLDH in leaf mitochondria from 30-days-old wild type, 8-14 and 5-13 transgenic lines detected by Western Blot using anti-L-GalLDH (Agrisera). Relative abundance, expressed as % of wild type signal, was obtained by densitometry. L-GalLDH activity (measured as rate of Cytc reduction) was determined in the mitochondria from 30-days-old wild type, 8-14 and 5-13 transgenic lines. Values represent means ± standard error and asterisks represent significant differences between inhibited and non-inhibited reactions analyzed by one-way ANOVA following by Tukey test (P < 0.05). Measurements from three independent mitochondrial preparations (n=3). **1C**. Rates of oxygen uptake SHAM-sensitive and NaN3-resistant (alternative respiration) determined in mitochondria from wild type, 8-14 and 5-13 transgenic lines. Asterisks represent significant differences of alternative respiration of transgenic leaf mitochondria when compared to wild type by one-way ANOVA following by Tukey test (P < 0.05). **1D**. Immunoblot of AOX detected when mitochondrial proteins are loaded without the reducing agent of free sulphydryl residues (2-mercaptoethanol) into sample buffer. A 66 kDa protein was detected by Western Blot using anti-AOX antibodies (Agrisera) in leaf mitochondria purified from 30-days-old wild type, 8-14 and 5-13 plants. Immunoblot of AOX (molecular weight of about 33 kDa) obtained when the reducing agent was added into sample buffer and subsequent detection with anti-AOX antibodies. Equal loading of gels was checked by Ponceau staining. Relative abundances were assessed by quantification of signals through densitometry and expressed as % of wild type level.

A Ascorbate production ($\mu g\ mg^{-1}\ protein^{-1}$) — Control, Azyde, SHAM, Antimycin, Rotenone, DPI

B L-GalLDH activity ($\mu mol\ Cytc.min^{-1}\ mg^{-1}\ protein^{-1}$) — Control, SHAM, Antimycin, Rotenone, DPI

C Ascorbate production ($\mu g\ mg^{-1}\ protein^{-1}$) — Green-mature, Fully ripe

L-GalLDH activity: Green-mature 0.51±0.006, Fully ripe 0.45±0.005

D Δ FAD Fluorescence (U) — Control, Azyde, SHAM, Antimycin, Rotenone, DPI

Figure 2A. Ascorbate production capacity measured in pure mitochondria treated or not with inhibitors (3 mM azyde, NaN3, 1mM SHAM, 2 μM antimycin A, 20 μM rotenone, and 5 mM DPI). Ascorbate synthesis was initiated in presence of 5 mM L-GalL. **2B**. Activity of L-GalLDH enzyme (assessed as capacity to reduce Cytc) determined in purified mitochondria incubated with 1mM SHAM, 2 μM antimycin A, 20 μM rotenone, and 5 mM DPI). Cytc reduction was started by adding 5mM L-GalL in presence of the Cytc oxidase inhibitor, azyde. **2C**. Ascorbate production and L-GalLDH activity determined in mitochondria from green-mature and full-ripe papaya fruit. **2D**. Ascorbate synthesis-dependent changes in flavin adenine dinucleotide (FAD) fluorescence measured in pure mitochondria incubated with the inhibitor compounds indicated above in figure 2A. AsA synthesis was started with 5mM L-GalL. Bars represent means ± standard error from at least three independent experiments.
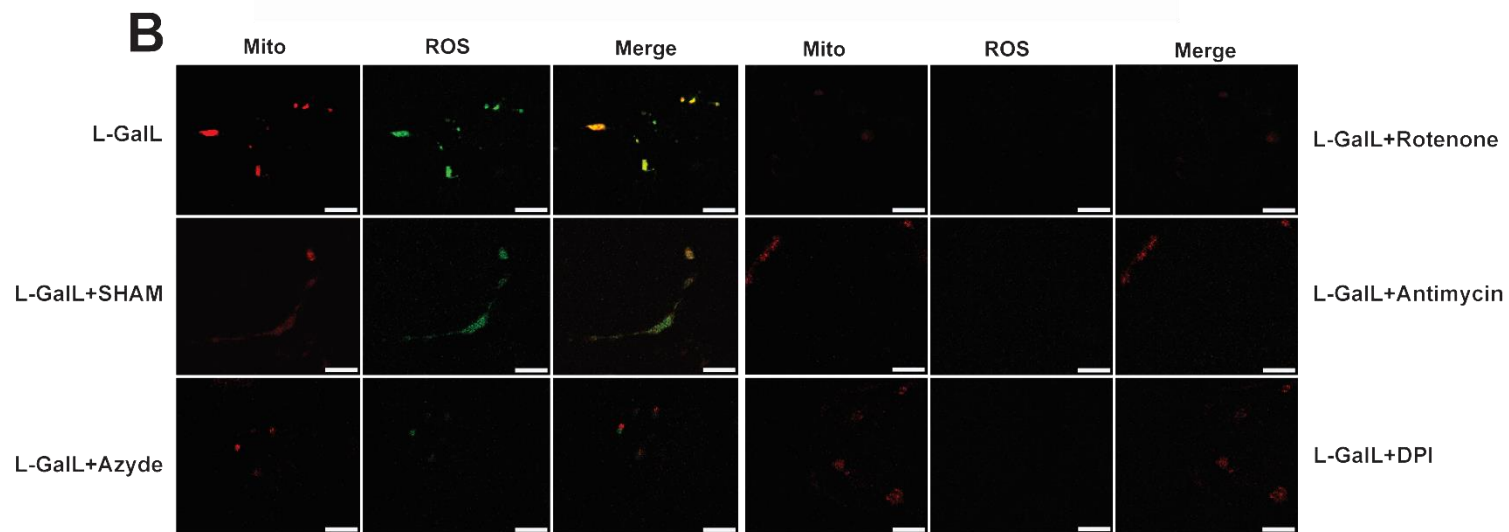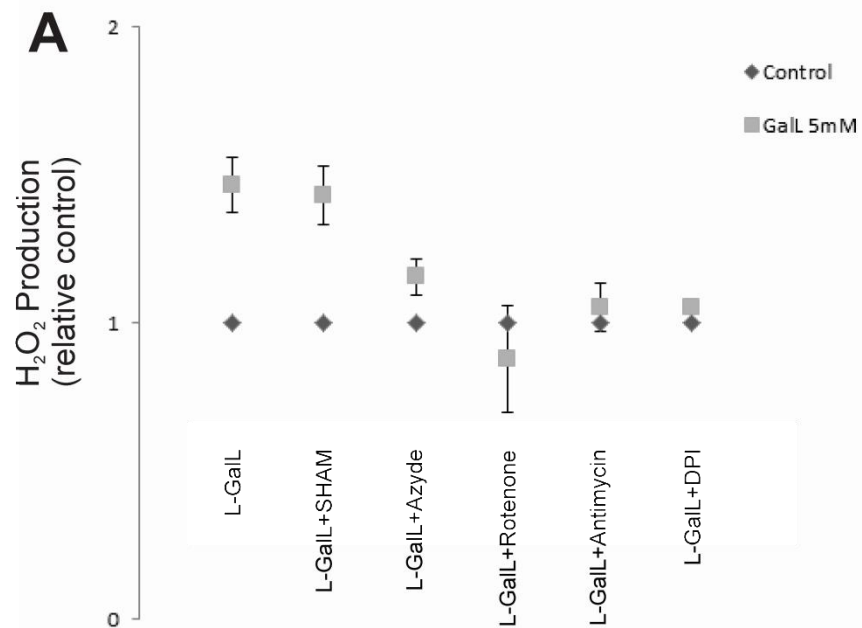
Figure 3A. Induction of hydrogen peroxide (H2O2) production by 5 mM L-GalL in pure mitochondria treated with 1 mM SHAM, 3 mM azyde, 20 μM rotenone, 2 μM antimycin A, and 5 mM DPI. H2O2 content was quantified using Amplex Red/horseradish peroxidase (HRP) assay and relative H2O2 level for all treatments was normalized to their corresponding controls without L-GalL. Bars are means ± standard error (n=3). **3B**. Representative confocal images of co-localization of ROS and mitochondria stains in fruit mesocarp tissue incubated with 5 mM L-GalL and the same inhibitor compounds as above. Mitochondria were localized with Mito-Tracker Red and ROS detection was performed with (2,7-dichlorodihydrofluorescein diacetate, DCF-DA). Scale bar 10 μm.
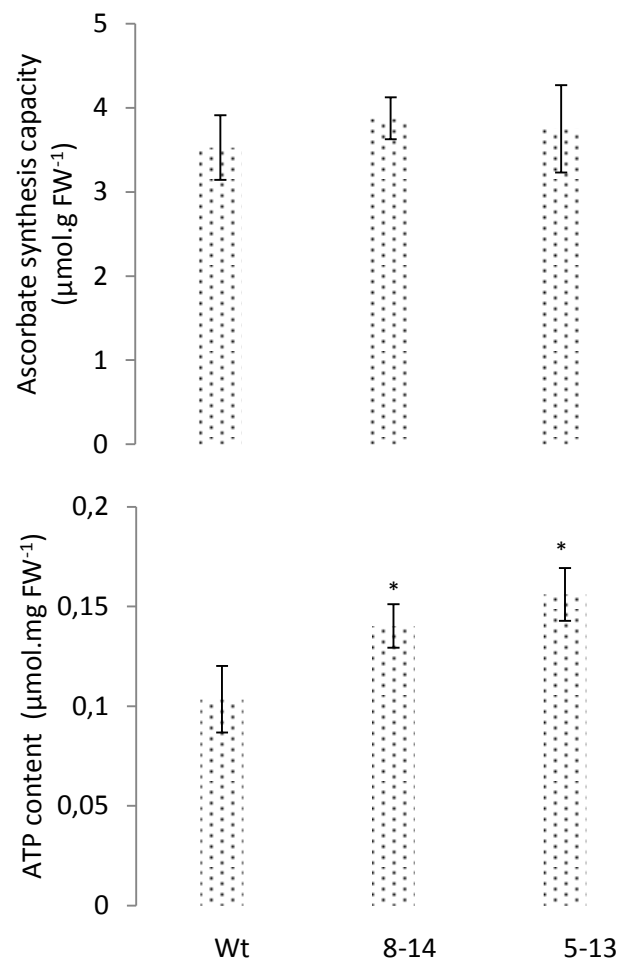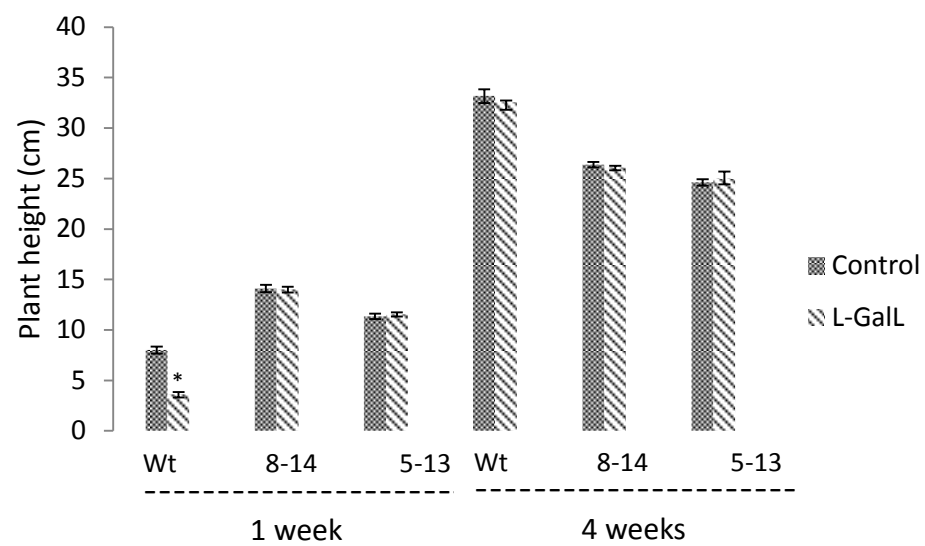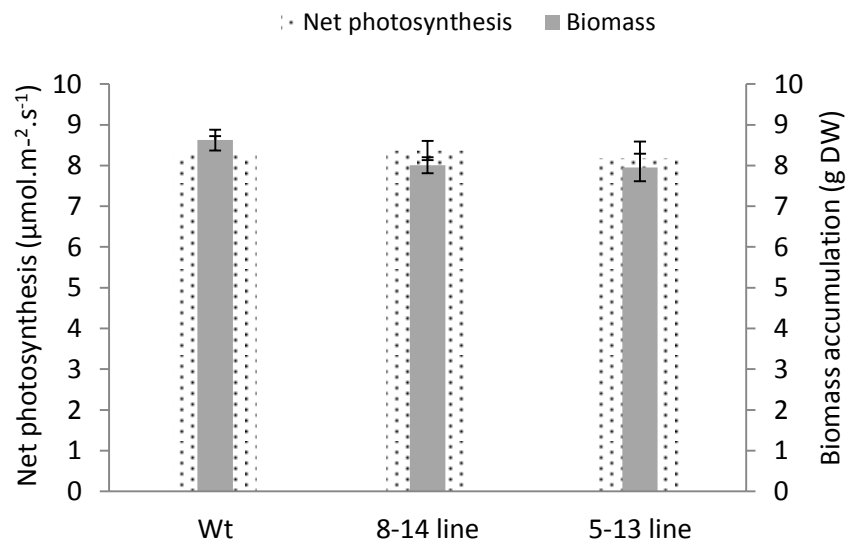
Figure 4A. Ascorbate synthesis capacity and ATP content of leaf tissue (in dark) determined in leaf tissue from four weeks-days-old wild type, 8-14 and 5-13 transgenic lines. **4B**. Effect of seed treatment with 20mM L-GalL on seedling growth from wild type, 8-14 and 5-13 transgenic lines measured one-week and four-weeks following the chemical treatment. **4C**. Net photosynthesis of fully expanded leaves (Dotted line) and dry weight of aboveground tissue (Grey line) determined in wild type, 8-14 and 5-13 transgenic lines at the four-weeks growth stage. All bars are means ± standard error from three independent experiments.

Parsed Citations

Alhagdow M, Mounet F, Gilbert L, Nunes-Nesi A, Garcia V, Just D, Petit J, Beauvoit B, Fernie AR, Rothan C, et al (2007) Silencing of the Mitochondrial Ascorbate Synthesizing Enzyme L-Galactono-1,4-Lactone Dehydrogenase Affects Plant and Fruit Development in Tomato. Plant Physiol 145: 1408–1422

Pubmed: Author and Title
Google Scholar: Author Only Title Only Author and Title

Arrigoni O, Calabrese G, De Gara L, Bitonti MB, Liso R (1997) Correlation between changes in cell ascorbate and growth of Lupinus albus seedlings. J Plant Physiol 150: 302–308

Pubmed: Author and Title
Google Scholar: Author Only Title Only Author and Title

Bartoli CG, Pastori GM, Foyer CH (2000) Ascorbate biosynthesis in mitochondria is linked to the electron transport chain between complexes III and IV. Plant Physiol 123: 335–44

Pubmed: Author and Title
Google Scholar: Author Only Title Only Author and Title

Bartoli CG, Yu J, Gómez F, Fernández L, McIntosh L, Foyer CH (2006) Inter-relationships between light and respiration in the control of ascorbic acid synthesis and accumulation in Arabidopsis thaliana leaves. J Exp Bot 57: 1621–1631

Pubmed: Author and Title
Google Scholar: Author Only Title Only Author and Title

Conesa A, Götz S, García-Gómez JM, Terol J, Talón M, Robles M (2005) Blast2GO: a universal tool for annotation, visualization and analysis in functional genomics research. Bioinforma Appl NOTE 21: 3674–3676

Pubmed: Author and Title
Google Scholar: Author Only Title Only Author and Title

Dahal K, Vanlerberghe GC (2017) Alternative oxidase respiration maintains both mitochondrial and chloroplast function during drought. New Phytol 213: 560–571

Pubmed: Author and Title
Google Scholar: Author Only Title Only Author and Title

Davletova S, Rizhsky L, Liang H, Shengqiang Z, Oliver DJ, Coutu J, Shulaev V, Schlauch K, Mittler R (2005) Cytosolic ascorbate peroxidase 1 is a central component of the reactive oxygen gene network of Arabidopsis. Plant Cell 17: 268–81

Pubmed: Author and Title
Google Scholar: Author Only Title Only Author and Title

Foyer CH, Kiddle G, Verrier P (2007) Transcriptional profiling approaches to understanding how plants regulate growth and defence: A case study illustrated by analysis of the role of vitamin C. Plant Syst. Biol. Birkhäuser Basel, Basel, pp 55–86

Pubmed: Author and Title
Google Scholar: Author Only Title Only Author and Title

Fricker MD, Meyer AJ (2001) Confocal imaging of metabolism in vivo: pitfalls and possibilities. J Exp Bot 52: 631–640

Pubmed: Author and Title
Google Scholar: Author Only Title Only Author and Title

Gleason C, Huang S, Thatcher LF, Foley RC, Anderson CR, Carroll AJ, Millar AH, Singh KB (2011) Mitochondrial complex II has a key role in mitochondrial-derived reactive oxygen species influence on plant stress gene regulation and defense. Proc Natl Acad Sci U S A 108: 10768–73

Pubmed: Author and Title
Google Scholar: Author Only Title Only Author and Title

Grillet L, Ouerdane L, Flis P, Hoang MTT, Isaure M-P, Lobinski R, Curie C, Mari S (2014) Ascorbate efflux as a new strategy for iron reduction and transport in plants. J Biol Chem 289: 2515–25

Pubmed: Author and Title
Google Scholar: Author Only Title Only Author and Title

Hao H-X, Khalimonchuk O, Schraders M, Dephoure N, Bayley J-P, Kunst H, Devilee P, Cremers CWRJ, Schiffman JD, Bentz BG, et al (2009) SDH5, a gene required for flavination of succinate dehydrogenase, is mutated in paraganglioma. Science 325: 1139–42

Pubmed: Author and Title
Google Scholar: Author Only Title Only Author and Title

Heringer AS, Reis RS, Passamani LZ, de Souza-Filho GA, Santa-Catarina C, Silveira V (2017) Comparative proteomics analysis of the effect of combined red and blue lights on sugarcane somatic embryogenesis. Acta Physiol Plant 39: 52

Pubmed: Author and Title
Google Scholar: Author Only Title Only Author and Title

Holtzapffel RC, Finnegan PM, Millar AH, Badger MR, Day DA (2002) Mitochondrial protein expression in tomato fruit during on-vine ripening and cold storage. Funct Plant Biol 29: 827

Pubmed: Author and Title
Google Scholar: Author Only Title Only Author and Title

Huang S, Millar AH (2013) Succinate dehydrogenase: the complex roles of a simple enzyme. Curr Opin Plant Biol 16: 344–349

Pubmed: Author and Title
Google Scholar: Author Only Title Only Author and Title

Keech O, Dizengremel P, Gardeström P (2005) Preparation of leaf mitochondria from Arabidopsis thaliana. Physiol Plant 124: 403–409
Pubmed: Author and Title
Google Scholar: Author Only Title Only Author and Title

Kotchoni SO, Larrimore KE, Mukherjee M, Kempinski CF, Barth C (2009) Alterations in the endogenous ascorbic acid content affect flowering time in Arabidopsis. Plant Physiol 149: 803–815
Pubmed: Author and Title
Google Scholar: Author Only Title Only Author and Title

Kozioł J (1971) [132] Fluorometric analyses of riboflavin and its coenzymes. Methods Enzymol 18: 253–285
Pubmed: Author and Title
Google Scholar: Author Only Title Only Author and Title

Kühn K, Yin G, Duncan O, Law SR, Kubiszewski-Jakubiak S, Kaur P, Meyer E, Wang Y, Small CC des F, Giraud E, et al (2015) Decreasing electron flux through the cytochrome and/or alternative respiratory pathways triggers common and distinct cellular responses dependent on growth conditions. Plant Physiol 167: 228–50
Pubmed: Author and Title
Google Scholar: Author Only Title Only Author and Title

Leferink NGH, Donald M, Jose F, Van Den Berg WAM, Van Berkel WJH (2009) Functional assignment of Glu386 and Arg388 in the active site of L-galactono-c-lactone dehydrogenase. FEBS Lett 583: 3199–3203
Pubmed: Author and Title
Google Scholar: Author Only Title Only Author and Title

Mailloux RJ, Harper M-E (2011) Uncoupling proteins and the control of mitochondrial reactive oxygen species production. Free Radic Biol Med 51: 1106–1115
Pubmed: Author and Title
Google Scholar: Author Only Title Only Author and Title

Mazorra LM, Senn ME, Grozeff GEG, Fanello DD, Carrión CA, Núñez M, Bishop GJ, Bartoli CG (2014) Impact of brassinosteroids and ethylene on ascorbic acid accumulation in tomato leaves. Plant Physiol Biochem 74: 315–322
Pubmed: Author and Title
Google Scholar: Author Only Title Only Author and Title

Millar AH, Whelan J, Soole KL, Day DA (2011) Organization and Regulation of Mitochondrial Respiration in Plants. Annu Rev Plant Biol 62: 79–104
Pubmed: Author and Title
Google Scholar: Author Only Title Only Author and Title

Mukherjee M, Larrimore KE, Ahmed NJ, Bedick TS, Barghouthi NT, Traw MB, Barth C (2010) Ascorbic Acid Deficiency in Arabidopsis Induces Constitutive Priming That is Dependent on Hydrogen Peroxide, Salicylic Acid, and the NPR1 Gene. Mol Plant-Microbe Interact 23: 340–351
Pubmed: Author and Title
Google Scholar: Author Only Title Only Author and Title

Noctor G, Foyer CH (2016) Intracellular Redox Compartmentation and ROS-Related Communication in Regulation and Signaling. Plant Physiol 171: 1581–92
Pubmed: Author and Title
Google Scholar: Author Only Title Only Author and Title

Noctor G, De Paepe R, Foyer CH (2007) Mitochondrial redox biology and homeostasis in plants. Trends Plant Sci 12: 125–134
Pubmed: Author and Title
Google Scholar: Author Only Title Only Author and Title

Nunes-Nesi A, Araújo WL, Fernie AR (2011) Targeting mitochondrial metabolism and machinery as a means to enhance photosynthesis. Plant Physiol 155: 101–107
Pubmed: Author and Title
Google Scholar: Author Only Title Only Author and Title

Ôba, K, Ishikawa S, Nishikawa M, Mizuno H, Yamamoto T (1995) Purification and Properties of L-Galactono-γ-Lactone Dehydrogenase, a Key Enzyme for Ascorbic Acid Biosynthesis, from Sweet Potato Roots. J Biochem 117: 120–124
Pubmed: Author and Title
Google Scholar: Author Only Title Only Author and Title

Oliveira JG, Mazorra LM, Silva GMC, da Cruz Saraiva KD, Santana DB, dos Santos CP, Oliveira MG, Costa JH (2017) Procedures of Mitochondria Purification and Gene Expression to Study Alternative Respiratory and Uncoupling Pathways in Fruits. Plant Respir. Intern. Oxyg. Humana Press, New York, NY, pp 143–165
Pubmed: Author and Title
Google Scholar: Author Only Title Only Author and Title

Oliveira MG, Mazorra LM, Souza AF, Silva GMC, Correa SF, Santos WC, Saraiva KDC, Teixeira AJ, Melo DF, Silva MG, et al (2015) Physiology Involvement of AOX and UCP pathways in the post-harvest ripening of papaya fruits. J Plant Physiol 189: 42–50

Pubmed: Author and Title
Google Scholar: Author Only Title Only Author and Title

Pineau B, Mathieu C, Gérard-Hirne C, De Paepe R, Chétrit P (2005) Targeting the NAD7 subunit to mitochondria restores a functional complex I and a wild type phenotype in the Nicotiana sylvestris CMS II mutant lacking nad7. J Biol Chem 280: 25994–26001
Pubmed: Author and Title
Google Scholar: Author Only Title Only Author and Title

Plumb W, Townsend AJ, Rasool B, Alomrani S, Razak N, Karpinska B, Ruban A V, Foyer CH (2018) Ascorbate-mediated regulation of growth, photoprotection, and photoinhibition in Arabidopsis thaliana. J Exp Bot 69: 2823–2835
Pubmed: Author and Title
Google Scholar: Author Only Title Only Author and Title

Ragan CI, Wilson MT, Darley-Usmar VM LP (1987) Sub-fractionation of mitochondria and isolation of the proteins of oxidative phosphorylation. IRL Press
Pubmed: Author and Title
Google Scholar: Author Only Title Only Author and Title

Renault G, Raynal E, Sinet M, Berthier JP, Godard B, Cornillault J (1982) A laser fluorimeter for direct cardiac metabolism investigation. Opt Laser Technol 14: 143–148
Pubmed: Author and Title
Google Scholar: Author Only Title Only Author and Title

Schertl P, Braun H-P (2014) Respiratory electron transfer pathways in plant mitochondria. Front Plant Sci 5: 163
Pubmed: Author and Title
Google Scholar: Author Only Title Only Author and Title

Schertl P, Sunderhaus S, Klodmann J, Grozeff GEG, Bartoli CG, Braun H-P (2012) L-galactono-1,4-lactone dehydrogenase (GLDH) forms part of three subcomplexes of mitochondrial complex I in Arabidopsis thaliana. J Biol Chem 287: 14412–9
Pubmed: Author and Title
Google Scholar: Author Only Title Only Author and Title

Schluepmann H, Pellny T, Dijken A van, Smeekens S, Paul M (2003) Trehalose 6-phosphate is indispensable for carbohydrate utilization and growth in Arabidopsis thaliana. Proc Natl Acad Sci 100: 6849–6854
Pubmed: Author and Title
Google Scholar: Author Only Title Only Author and Title

Selinski J, Hartmann A, Deckers-Hebestreit G, Day DA, Whelan J, Scheibe R (2018) Alternative Oxidase Isoforms Are Differentially Activated by Tricarboxylic Acid Cycle Intermediates. Plant Physiol 176: 1423–1432
Pubmed: Author and Title
Google Scholar: Author Only Title Only Author and Title

Smirnoff N (2018) Ascorbic acid metabolism and functions: A comparison of plants and mammals. Free Radic Biol Med 122: 116–129
Pubmed: Author and Title
Google Scholar: Author Only Title Only Author and Title

Smirnoff N (2011) Vitamin C: The Metabolism and Functions of Ascorbic Acid in Plants. Adv Bot Res 59: 107–177
Pubmed: Author and Title
Google Scholar: Author Only Title Only Author and Title

Subbarow CHF and Y (1925) The colorimetric determination of phosphorus. J Chem Inf Model 6: 375–400
Pubmed: Author and Title
Google Scholar: Author Only Title Only Author and Title

Sweetlove LJ, Beard KFM, Nunes-Nesi A, Fernie AR, Ratcliffe RG (2010) Not just a circle: Flux modes in the plant TCA cycle. Trends Plant Sci 15: 462–470
Pubmed: Author and Title
Google Scholar: Author Only Title Only Author and Title

Tamaoki M, Mukai F, Asai N, Nakajima N, Kubo A, Aono M, Saji H (2003) Light-controlled expression of a gene encoding l-galactono-γ-lactone dehydrogenase which affects ascorbate pool size in Arabidopsis thaliana. Plant Sci 164: 1111–1117
Pubmed: Author and Title
Google Scholar: Author Only Title Only Author and Title

Umbach AL, Ng VS, Siedow JN (2006) Regulation of plant alternative oxidase activity: A tale of two cysteines. doi: 10.1016/j.bbabio.2005.12.005
Pubmed: Author and Title
Google Scholar: Author Only Title Only Author and Title

Vanlerberghe GC (2013) Alternative Oxidase: A Mitochondrial Respiratory Pathway to Maintain Metabolic and Signaling Homeostasis during Abiotic and Biotic Stress in Plants. Int J Mol Sci 14: 6805–6847
Pubmed: Author and Title
Google Scholar: Author Only Title Only Author and Title

Vanlerberghe GC, Martyn GD, Dahal K (2016) Alternative oxidase: a respiratory electron transport chain pathway essential for

maintaining photosynthetic performance during drought stress. Physiol Plant 157: 322–337

Pubmed: Author and Title
Google Scholar: Author Only Title Only Author and Title

Wagner AM, Wagner MJ (1995) Measurements of in Vivo Ubiquinone Reduction Levels in Plant Cells. Plant Physiol 108: 277–283

Pubmed: Author and Title
Google Scholar: Author Only Title Only Author and Title

Westlake TJ, Ricci WA, Popescu G V, Popescu SC (2015) Dimerization and thiol sensitivity of the salicylic acid binding thimet oligopeptidases TOP1 and TOP2 define their functions in redox-sensitive cellular pathways. Front Plant Sci 6: 327

Pubmed: Author and Title
Google Scholar: Author Only Title Only Author and Title

Yamamoto Y, Kobayashi Y, Devi SR, Rikiishi S, Matsumoto H (2002) Aluminum toxicity is associated with mitochondrial dysfunction and the production of reactive oxygen species in plant cells. Plant Physiol 128: 63–72

Pubmed: Author and Title
Google Scholar: Author Only Title Only Author and Title

Yoshida K, Shibata M, Terashima I, Noguchi K (2010) Simultaneous Determination of In Vivo Plastoquinone and Ubiquinone Redox States by HPLC-Based Analysis. Plant Cell Physiol 51: 836–841

Pubmed: Author and Title
Google Scholar: Author Only Title Only Author and Title

Yuan L-B, Dai Y-S, Xie L-J, Yu L-J, Zhou Y, Lai Y-X, Yang Y-C, Xu L, Chen Q-F, Xiao S (2017) Jasmonate Regulates Plant Responses to Postsubmergence Reoxygenation through Transcriptional Activation of Antioxidant Synthesis. Plant Physiol 173: 1864–1880

Pubmed: Author and Title
Google Scholar: Author Only Title Only Author and Title